NASA CR-132389

METAL-WOOL HEAT SHIELDS FOR SPACE SHUTTLE

By

Robert C. Miller and John L. Clure

MARCH 1974

Prepared under Contract No. NAS1-12427 by

Hughes Helicopters division of summa corporation / culver city, california

for

NATIONAL AERONAUTICS AND SPACE ADMINISTRATION

NASA CR-132389

METAL-WOOL HEAT SHIELDS FOR SPACE SHUTTLE

By Robert C. Miller and John L. Clure

Prepared under Contract No. NAS1-12427 by

HUGHES HELICOPTERS Division of Summa Corporation
Culver City, California

for

NATIONAL AERONAUTICS AND SPACE ADMINISTRATION

For sale by the Office of Technical Services, Department of Commerce:
Washington, D. C. 20230--Price $0. 75

Page Intentionally Left Blank

CONTENTS

CONTENTS (CONT)

METAL-WOOL HEAT SHIELDS FOR SPACE SHUTTLE

By Robert C. Miller and John L. Clure

SUMMARY

The packaging of metal wool for reusable thermal heat shields applied to aerodynamic and other surfaces for the Space Shuttle was analyzed and designed, and samples were fabricated and experimentally studied. Parametric trends were prepared for selected configurations.

An all-metal, thermally efficient, reliable, reusable and producible heat shield system was designed and structurally tested for use on spacecraft aerodynamic surfaces where temperatures do not exceed 810°K (1000°F). Type 300 series stainless steel heat shields are considered practical to temperatures of 1250°K (1790°F) when spacecraft flight profiles result in low aerodynamic loads concomitant with low oxygen concentration.

Stainless steel sheet, corrugated primarily for structure and secondarily in the transverse plane for thermal expansion, was shown to accommodate thermal expansion in all directions when restrained at the edges and heated to 1360°K (1990°F). Aerodynamic loads of 0.35×10^5 newtons/meter^2 (5 psi), and higher, may be easily accepted by structures of this design.

Seven all-metal thermal protection specimens, 12.7 cm square and 2.5 cm thick (packaged density variation from 61.4 to 84.7 kg/meter^3, 3.8 to 5.3 lb/ft^3), were fabricated and are being experimentally evaluated at simulated shuttle entry conditions in an arc jet facility at the Langley Research Center. The arc jet test results will be reported by NASA at a later date. From very preliminary testing at NASA, the metal-wool concept looks very promising.

INTRODUCTION

Thermal protection is required for portions of the exterior surfaces of the Space Shuttle orbiter and future high-altitude hypersonic aircraft. Porous ceramic materials such as silica (S_iO_2) and mullite ($3\,Al_2O_3 \cdot 2\,S_iO_2$), bonded to the spacecraft structures in tiles, have been utilized and are representative of the current state of the art (reference 1).

The packaging of a metal-wool insulation was undertaken to make available the desirable thermal and structural properties of such a system. Metal wool is inherently resistant to damage by impact, is low in weight, resists chemical reaction with its service environment, and is thermally competitive with the best insulations. The low thermal conductivity of metal-wool systems is illustrated and compared with other high-performance insulations in figure 1.

An all-metal thermal protection system offers an alternate and attractive solution to the complex insulation problems associated with high-speed flight and spacecraft.

The thermal conductivity of metal-wool insulation in the 4- to 25-micron filament range and its performance as an insulation was established in prior laboratory studies and by field performance (references 2, 3, and 4). Metal wool has demonstrated a high tolerance for vibrational and high G environments in the presence of exhaust products, and this insulation system was initially developed for the rotor blade hot-gas duct of a large pressure jet helicopter. Jet engine exhaust gas at a temperature of 870°K flowed through a 16.8-meter-long rotor blade to provide propulsive force at the blade tip for this aircraft propulsion system.

The work performed in this study was addressed to the design of thermal-expansion-controlled aerodynamic skins, their attachment to the aircraft structure, the methodology of manufacture, and the containment (packaging) of the metal-wool thermal insulation to provide an efficient and low-weight barrier to aerodynamic heating of aircraft structures. A sketch of the configuration evolved in this program is shown in figure 2.

Physical quantities in this paper are given in the International System of Units (SI), but they were measured in U.S. Customary Units. Factors relating the two systems are given in reference 5 and the following table.

CONVERSION TABLE FOR UNITS USED IN THIS REPORT

To convert from	To	Multiply by
cm	inch	0.3937
°K	°R	1.8
radian	degree	57.296
N/m	$lb_f/in.$	5.71×10^{-3}
N/m^2	$lb_f/in.^2$	1.45×10^{-4}
$N\text{-}m^2$	$lb_f\text{-}in.^2$	3.48×10^{2}
kg/m^2	lb_m/ft^2	0.2048
kg/m^3	lb_m/ft^3	0.0624

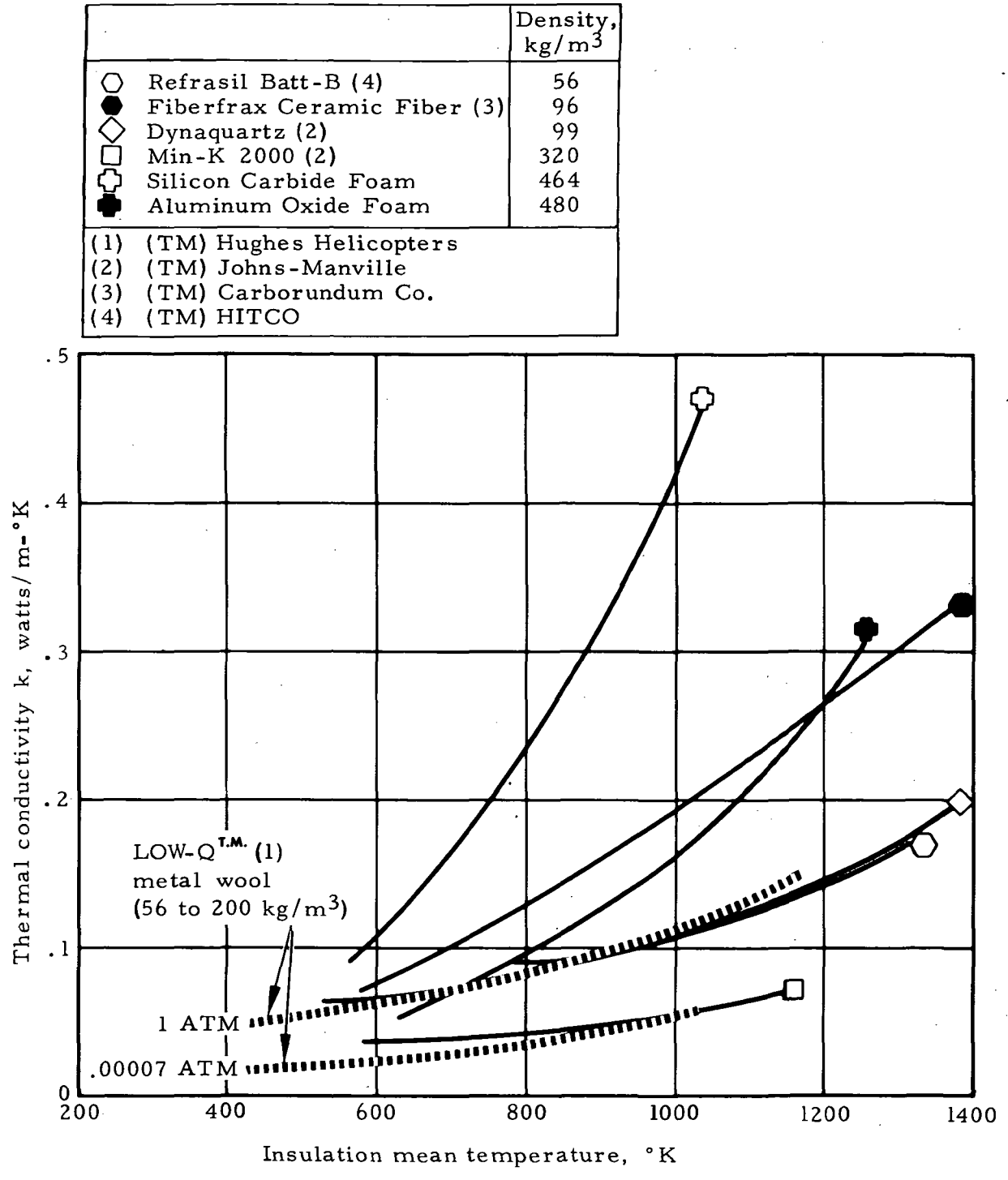

Figure 1. - Comparison of metal-wool thermal conductivity with a range of insulation products.

SYMBOLS AND UNITS

b	Beam width, cm
E	Modulus of elasticity, newtons/meter^2, N/m^2
E'	Effective modulus of elasticity, newtons/meter^2, N/m^2
I	Moment of inertia, cm^4
k	Thermal conductivity, watts/meter-°K, W/m-°K
Δk	Thermal short, watts/meter-°K per meter^2 of surface area
P	Corrugation pitch, cm
t	Thickness, cm
w	Aerodynamic pressure, newtons/meter^2, N/m^2
W	Concentrated load, newtons, N
x, y	Rectangular Cartesian coordinates
y	Corrugation depth, cm
y_o	Distance from neutral axis to outer fiber, cm

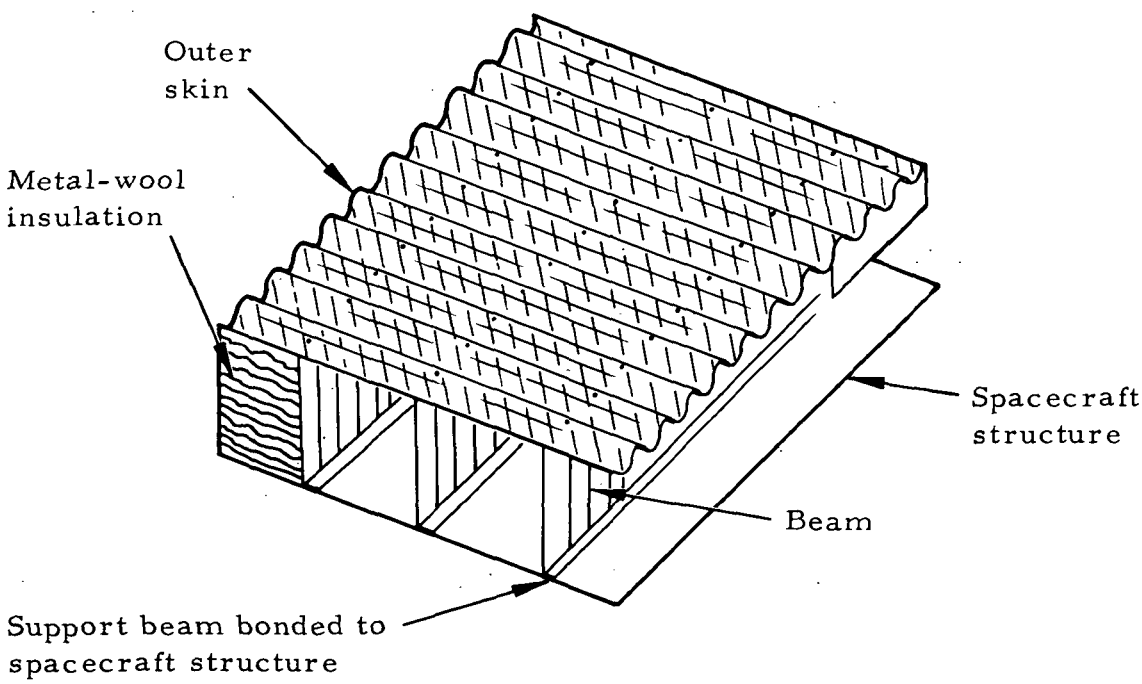

Figure 2. - Schematic of a metal-wool insulation packaged by a single-element skin fastened to the spacecraft structure by lineal beam corrugated sheet supports.

PRELIMINARY DESIGN

The primary study element in the program was the structure necessary to satisfy the aerothermal environment of an aircraft surface. The structure provided basically satisfied the following criteria:

a. Maintain aerodynamic and/or gas pressure loads with acceptable distortion

b. Keep to a minimum thermal shorts from aerodynamic skin to aircraft structure

c. Accommodate thermal expansion

d. Perform at the service temperature

e. Prevent ambient air flow into the insulation, or any flow in the insulation system

f. Vent insulation to minimize skin loads and maximize insulation efficiency

Decisions that would strongly determine the success of the program were made in the initial stages of study. Controlling parameters that were identified and reviewed are discussed in the following paragraphs.

Material Selection

Materials that included stainless steel, aluminum, brass, silicones, and polyamides were evaluated, and the 300 series stainless steels were selected. Stainless steel permits high-strength, low-weight designs which can perform in a temperature range from 20°K to 1250°K and which offer a greater versatility. Advantages offered by materials other than stainless steel were found to be limited to specific temperature regimes, and studies for limited service were not justified by the scope of the program.

Material Configuration

Concepts utilizing metal screen, sheet metal, and screen/sheet metal combinations were studied, and sheet stainless steel was selected as the most viable configuration based on structural efficiency and weight. Sheet metal in thicknesses of 0.00127, 0.00254, 0.00381, and 0.00508 cm and thicker is commercially available and lends itself to practical fabrication

methods. A skin may be fabricated from sheet metal and, through appropriate design, thermal expansion may be effectively accommodated. The skin is of inherent low permeability and can be made in gas-tight sections, tiles, or blankets by employing quality controls, necessary pressure tests, and sealing if openings are found. Openings may be sealed by employing either local inert gas welding or high-temperature soldering techniques.

Thermal Expansion Accommodation

Stainless steel sheet in the commercially available thickness range from 0.00127 to 0.00508 cm was configured and experimentally demonstrated to accommodate thermal expansion in all directions. Micro corrugations of sinusoidal shape were oriented at $\pi/4$ radian to larger corrugations. The micro corrugations provide for thermal expansion in one direction while the large or major corrugations control thermal expansion in a plane normal to the micro corrugations. Additionally, the major corrugations increase the sheet structural strength in the longitudinal plane of the corrugations.

Manufacturing Methodology

The micro corrugations were formed in the metal by placing the sheet in a press where a male die in combination with a rubber sheet was used to deform the metal. The metal sheet with micro corrugations was then run through a matched set of gears to form the major corrugations without damage to the micro corrugations. Each size of major corrugation required a specific gear set size.

Pulse, electron beam, laser beam, and ultrasonic welding techniques were investigated and demonstrated. Electron and laser beam welding were found to be impractical, and ultrasonic welding required development beyond the scope of the program. Pulse (capacitor discharge) welding was selected as the preferred joining method for study.

Aerodynamic Skin Options

Aerodynamic surfaces on large hypersonic aircraft flying at high altitudes will experience a thick boundary layer, and this environment may not require the airfoil surface smoothness traditionally specified. A smooth-surface skin may be provided, if required, by either a thin metal sheet joined to the substructure by pulse welds or by a sheet which has been double-micro-corrugated. A thin sheet will not transmit thermal growth effectively in the flat plane of the sheet and will tend to deform

without specific manufactured discontinuities in the plane of expansion. Four designs that were examined are presented in figure 3. The double-micro-corrugated configuration was selected as the preferred approach.

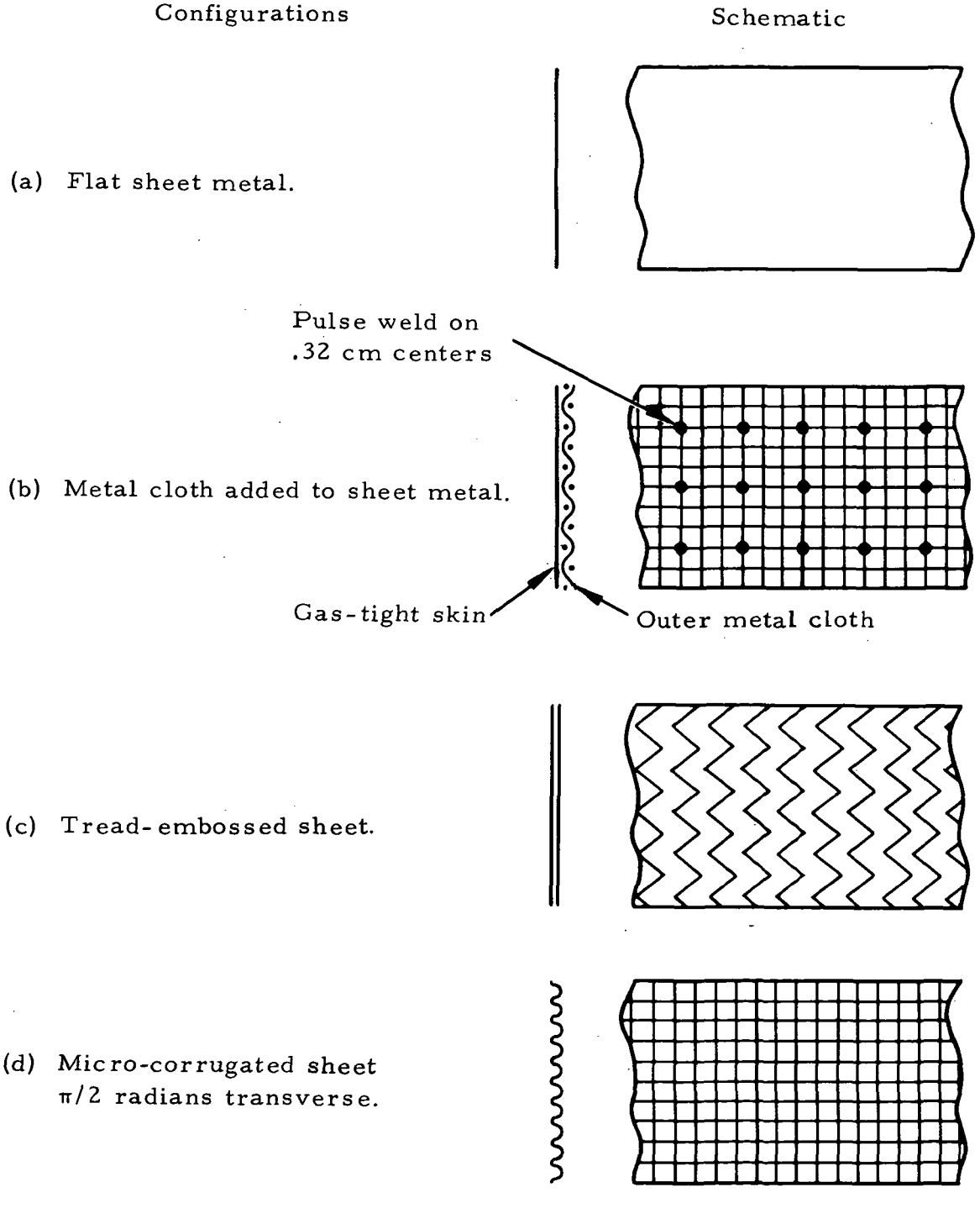

Figure 3. - Schematic of aerodynamic skin configuration options.

Structural Selection

Structural corrugations in a sheet provide strength in one direction only, therefore a single-element skin of this design must depend on the support system for stiffness in the direction normal to the corrugations. A skin structure having equal stiffness in all directions is obtained from two elements whose structural corrugation are oriented normal to each other.

Major corrugations in a size range from 0.165 cm to 0.51 cm in depth were selected for skin structure skins in single and cross-ply orientation. The effects of sheet metal thickness, micro-corrugation orientation and additional skin layers were defined by the experimental results. The systems are schematically illustrated in figure 4.

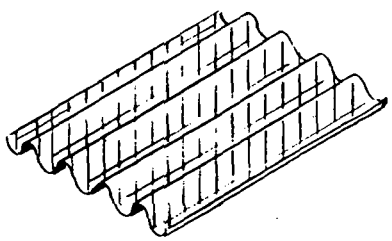

Single element.

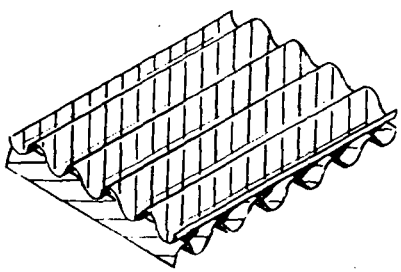

Double-element cross-ply layup.

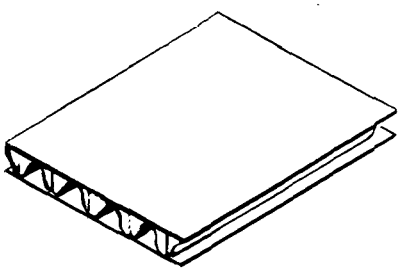

Single element with top and bottom skins.

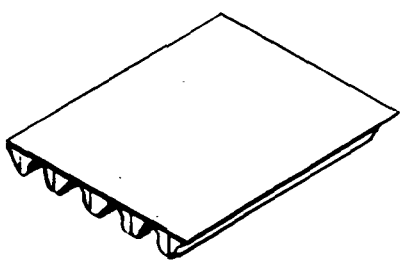

Single element with top aerodynamic skin.

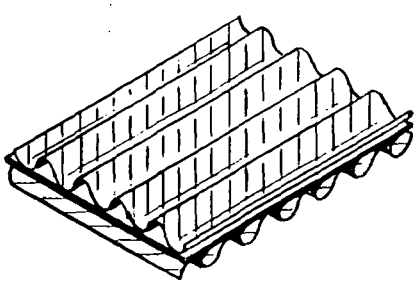

Double-element cross-ply layup with center diaphragm.

Note: All skin designs have micro corrugations oriented at $\pi/4$ radians to major corrugations.

Figure 4. - Schematic of candidate skin structures.

The support structure from the aerodynamic skin to the spacecraft structure was studied, and the most efficient supports based on weight and thermal short considerations were hollow circular columns or lineal ribbons, each formed from stainless steel sheet metal which had been corrugated to increase column strength. These configurations were initially defined by analysis, and later experimentally, to arrive at a preferred skin-support system configuration. The two candidate designs that resulted from the preliminary design study are illustrated in figure 5.

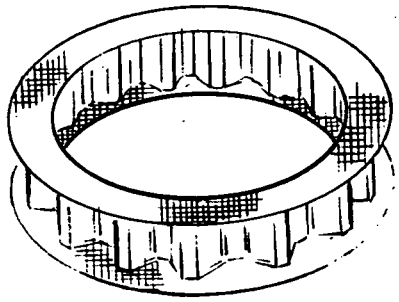

Circular hollow column support* for use with omnidirectional skin structure.

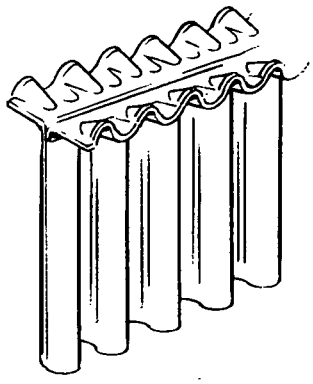

Lineal beam column support* for use with unidirectional skin structure.

Figure 5. - Candidate support structure designs.

*Patent applied for by Hughes Helicopters, division of summa corporation.

Joints

Methods for joining metal heat-shield panels or sections and methods for joining ceramic tiles and metal systems were evaluated and are discussed in appendix A.

Thermal Short Reduction

Design practice that offers a minimum heat leak from the outer skin to the spacecraft structure was reviewed, and recommendations are presented in appendix B.

Venting of Insulation System

Metal wool offers an inherent advantage of reduced insulation thermal conductivity at space and near-space pressures, and venting of the insulation system to ambient pressure greatly reduces the structural loads on the heat-shield structure. The low thermal conductivity of metal-wool systems at sea level is reduced by a factor of approximately three by reducing the ambient pressure in the insulation to space vacuum. This pressure effect is significant to altitudes as low as 46 kilometers.

A spacecraft insulation system may be vented to ambient with attention directed to the following (or equal) procedures:

1. Vents sealed with fail-safe frangible discs while on pad or in storage.

2. Open vents before launch (discs will fail at low altitude after launch).

Analysis

The analytical methods used to evaluate design and correlate data are summarized in appendix C. Standard accepted techniques were applied in the analysis and data evaluation.

EXPERIMENTAL STUDIES

The accommodation of thermal expansion in a double corrugated metal sheet was demonstrated early in the program in advance of the fabrication of more complex specimens and subsequent tests.

A steel block test fixture, 7.62 x 12.7 x 3.8 cm thick, with an opening of 3.81 x 7.62 cm through the full thickness of the block, was used to constrain the corrugated element thermal test specimen as illustrated in figure 6.

The test specimen was welded to the steel block to provide a more severe restraint to thermal expansion than is judged to exist under actual service and was torch-heated to the 1260-1370°K range. The test temperature was verified with a shielded thermocouple, and the test item was found to retain its structural integrity after four heating cycles.

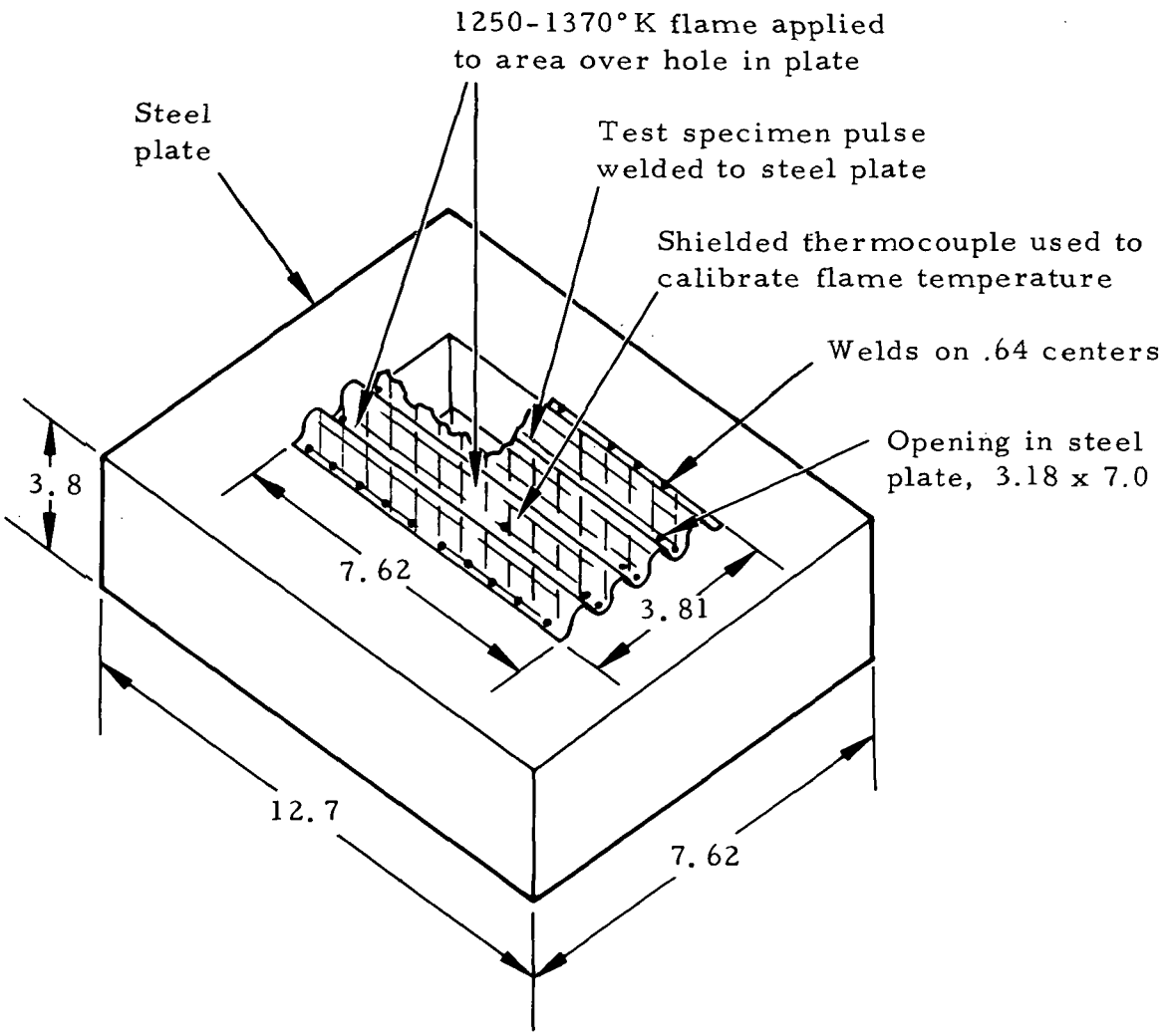

Note: All dimensions are in centimeters.

Figure 6. - Schematic of test fixture to evaluate thermal expansion capability of a double corrugated unidirectional skin element.

The structural properties of selected elements and combinations of elements were established in a series of bending tests where simply supported beam specimens approximately 3.8 cm wide by 15.2 cm long were subjected to a concentrated load. The study was designed to provide parametric data on sheet metal thickness, configuration, weight, and thermal short characteristics.

The orientation, depth, and population of micro corrugations with respect to the major corrugations were studied, and 9.84 per cm with a depth displacement of 0.0038 cm was selected for all skin structure specimens. Figure 7 presents photographs of micro corrugations oriented at

(a) Micro corrugations at $\pi/6$ radian to major corrugations.

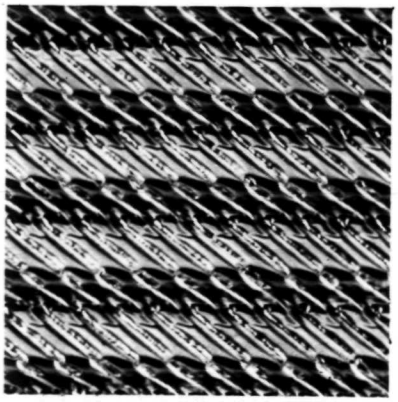

(b) Micro corrugations at $\pi/4$ radian to major corrugations.

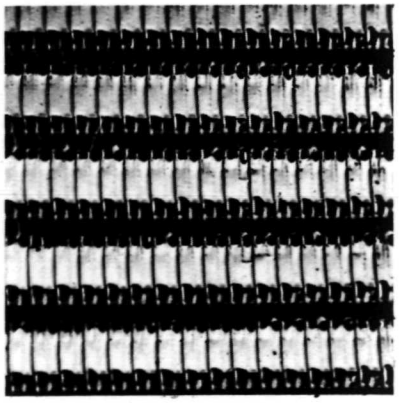

(c) Micro corrugations normal to major corrugations.

Figure 7. - Thermal-expansion-controlled skin configurations with combined major and micro corrugations.

$\pi/6$, $\pi/4$, and $\pi/2$ radians to major structural corrugations. These preliminary samples verified the manufacturing technique, and from them the $\pi/4$ radian orientation was selected for all specimens.

Experimental results are presented in the following paragraphs, with each selected structural system as the primary variable and with other parameters as secondary variables.

Single-Element Unidirectional-Strength Skin

Three major corrugation sizes were selected to parametrically evaluate the effect of corrugation depth on structural properties. A metal thickness range of 0.00254, 0.00381, and 0.00508 was selected for the study.

A photograph of each of the three corrugation sizes for a sheet metal thickness of 0.00254 cm is presented in figure 8, and the specimens studied are described in table I.

TABLE I.– SINGLE-STRUCTURAL-ELEMENT SKIN SPECIMEN PARAMETERS

Item	Number of corrugations per cm	Corrugation depth, cm	Sheet metal thickness, cm
1	2.6	0.165	0.00254, 0.00381, and 0.00508 for all specimens
2	1.34	0.338	
3	0.98	0.51	

The analytical predictability of the stiffness parameter (EI) was verified by experimentally measuring the beam deflection of sheet metal which had been stiffened by structural corrugations. Three metal thicknesses and three corrugation sizes were tested and showed the excellent agreement with analysis illustrated in figure 9.

The accepted value for the modulus of elasticity for stainless steel ($E = 193$ giga N/m^2) was used in the analysis, and, with this known value, the section moment of inertia was obtained from the experimental data. The moment of inertia for the section was also determined by the accepted analytical methods described in appendix C.

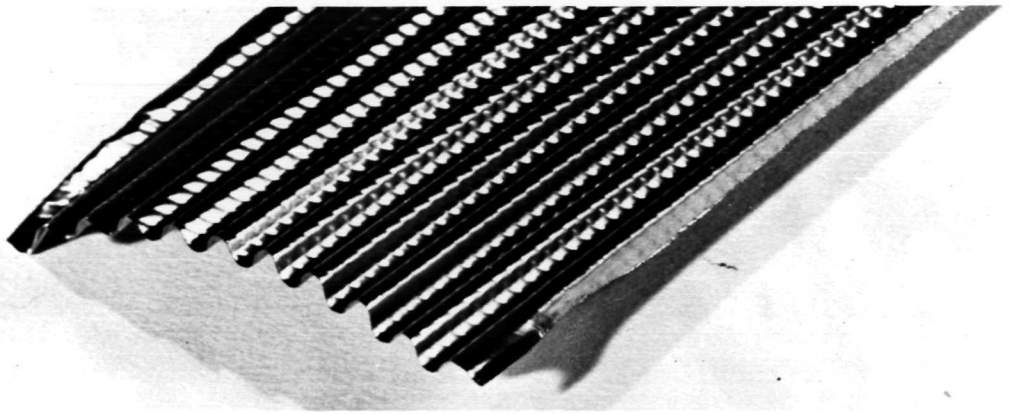

(a) 2.6 major corrugations per cm, .165 cm deep, micro corrugations .0038 cm deep.

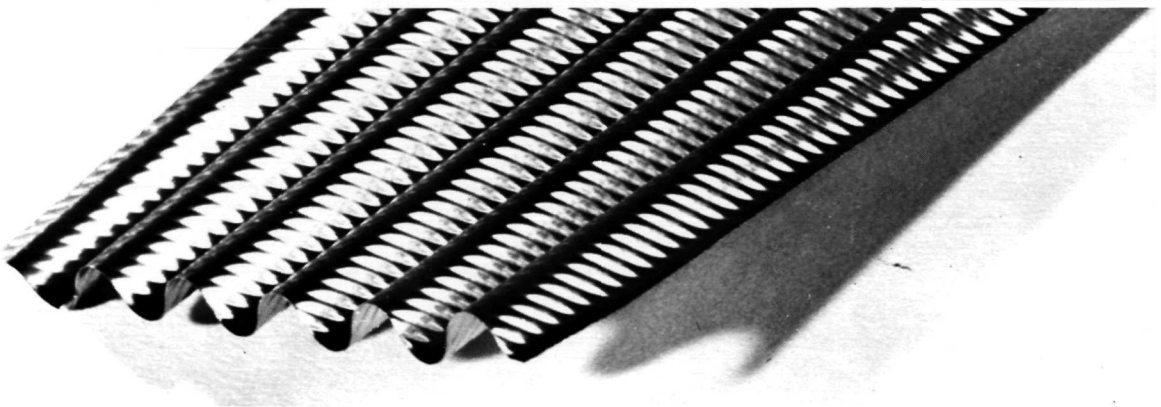

(b) 1.34 major corrugations per cm, .338 cm deep, micro corrugations .0038 cm deep.

(c) .98 major corrugations per cm, .51 cm deep, micro corrugations .0038 cm deep.

Figure 8. - Single-element unidirectional structure 0.00254 cm thick sheet stainless steel with micro corrugations at $\pi/4$ radian to major corrugations.

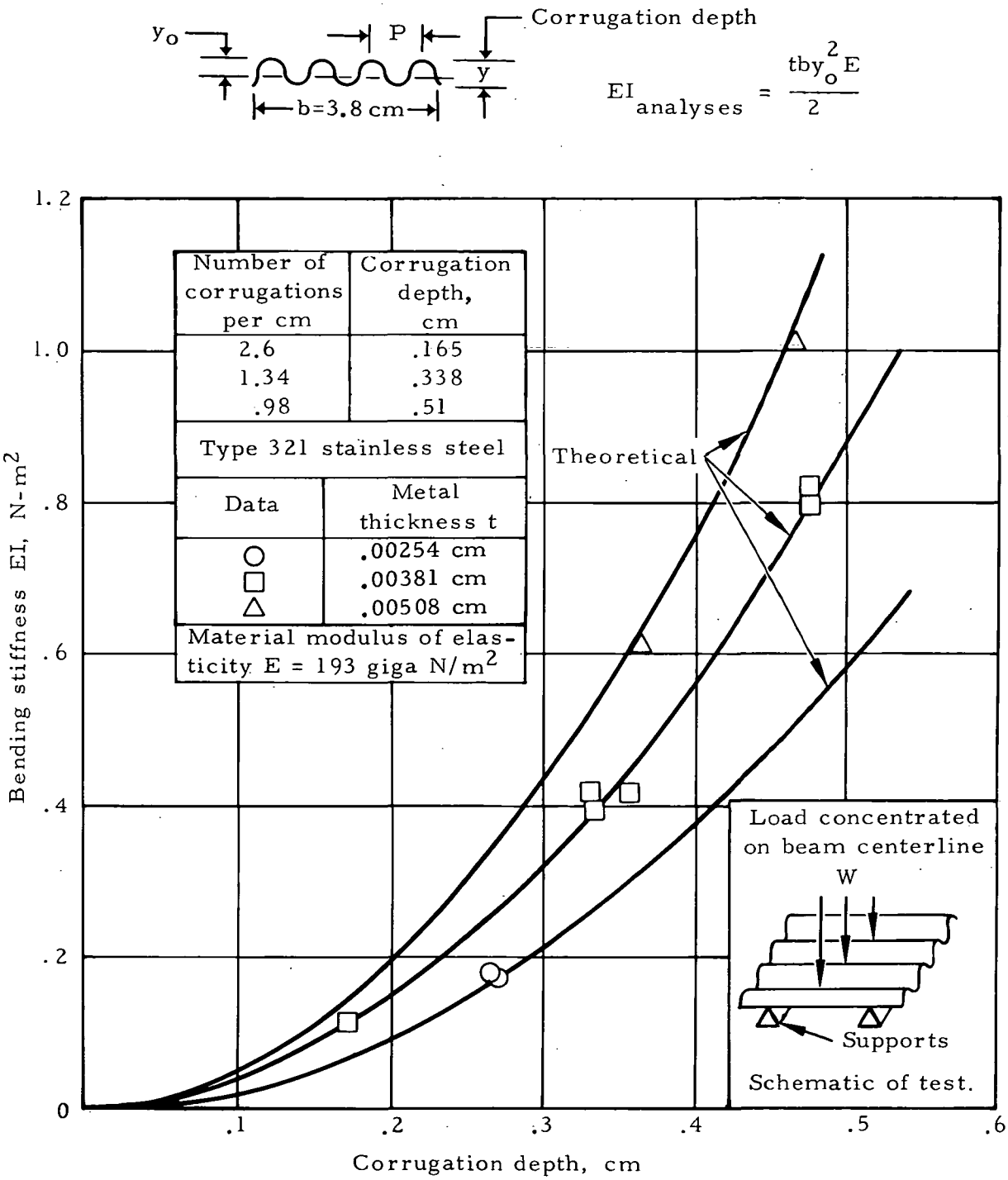

Figure 9. - Comparison of analytical and experimental beam stiffness for corrugated beams without micro corrugations.

It was hypothesized that the addition of micro corrugations would not alter the moment of inertia of a corrugated beam, since the metal distribution about the axis of reference is identical to that of a flat-sheet corrugated beam. However, the stiffness of the beam was altered by micro corrugations aligned at transverse angles to the major corrugations. The complexity of a structure with micro and major corrugations did not permit an analytical prediction; therefore, beam stiffness was experimentally determined for the three major corrugation sizes for a range of foil thickness and with micro corrugations aligned at $\pi/4$ radians to the major corrugations. The deviation from the stiffness obtained without micro corrugations is shown in figure 10. The reduction in the stiffness ratio, as shown in figure 10, is affected both by the metal thickness and the major corrugation depth. The overall effect of the micro corrugations on beam stiffness is shown in figure 11 where it is seen that the rate of change in stiffness increases with increase in the major corrugation depth. However, a stiffer beam is still realized with an increase in major corrugation depth.

Additional beam bending tests were conducted to determine the strength/weight effect of adding a top aerodynamic skin to a single element and also a top and bottom skin. The results obtained are summarized in table II. The beam specimens with a top aerodynamic skin showed no improvement in strength over the specimens without a skin. Theoretically an increase in strength of approximately 2.2 should have been realized. It was hypothesized that the intermittent weld attachment technique used to fasten the skin to the corrugated element prevented the top sheet from carrying or supporting any load. The use of this type of attachment is mandatory to accommodate thermal expansion. Thus, any requirement for an aerodynamic skin will result in a weight penalty.

The addition of a top and bottom skin resulted in an approximately 60-percent improvement over single-element strength, but at the expense of a 48-percent increase in weight per unit strength. For the same reasons given for the top skin, the full theoretical strength of a box structure was not realized.

Double-Element Omnidirectional-Strength Skin

Data was obtained with a double-element, corrugated sheet metal beam system, with the main structural elements aligned normal to each other to offer a structure of omnidirectional strength suitable for use with point or column supports. Photographs of the specimens studied are presented in figure 12 and are additionally described in table III.

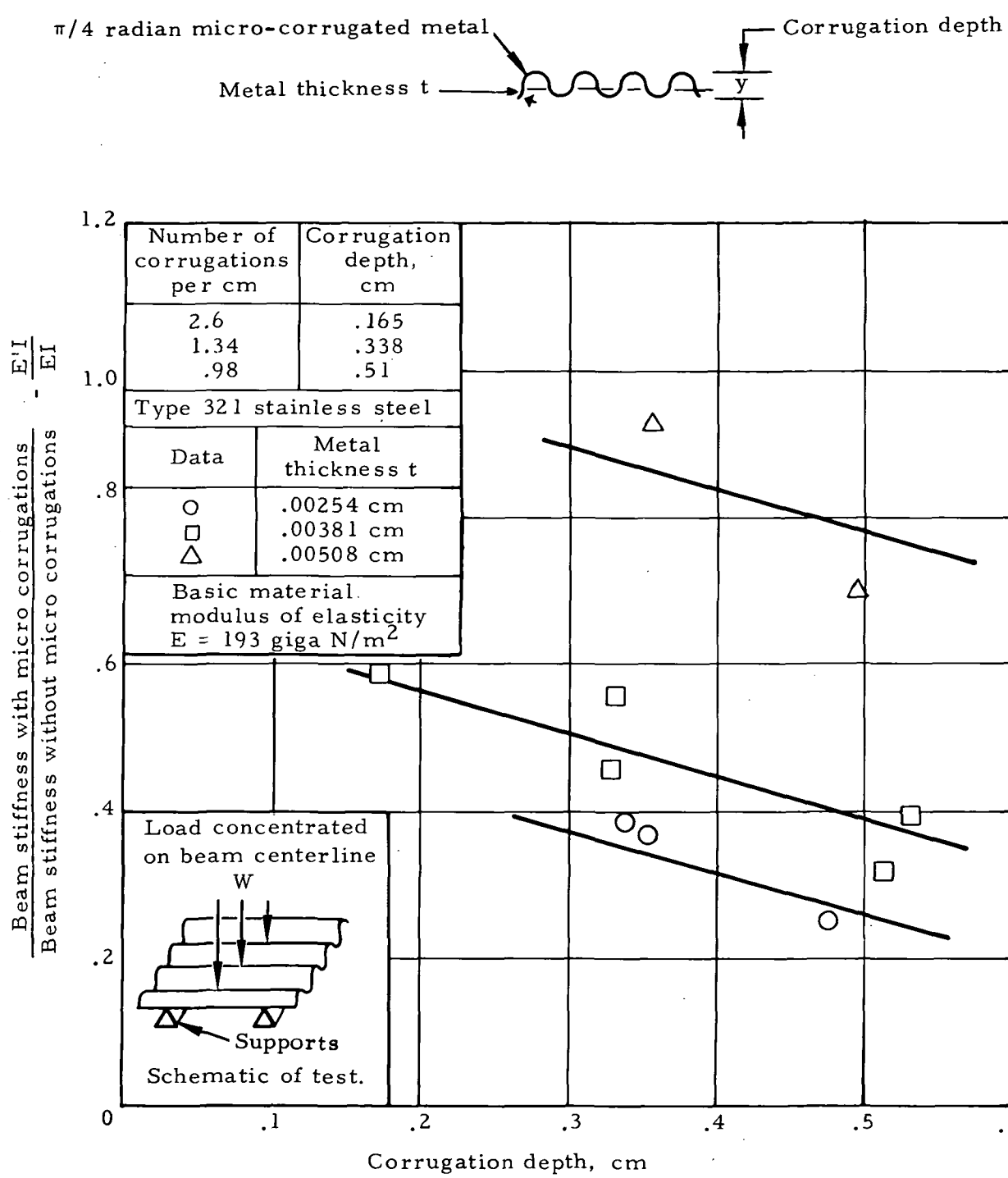

Figure 10. - Experimentally determined beam stiffness of a single-element unidirectional corrugated beam as functions of corrugation depth and metal thickness, with π/4 radian micro corrugations of 0.0038 cm depth.

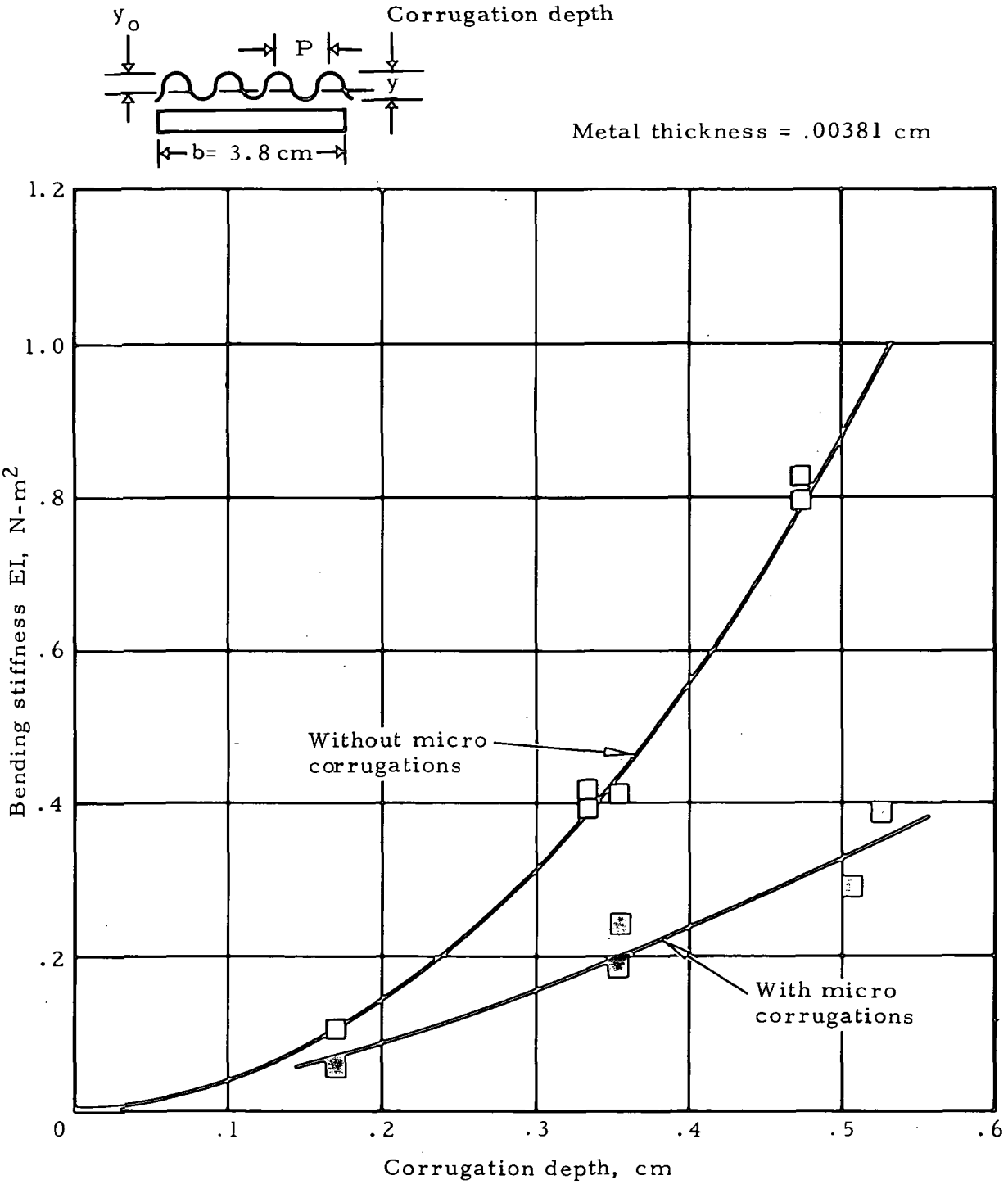

Figure 11. - Comparison of beam stiffness for corrugated beams with and without micro corrugations.

TABLE II.– UNIDIRECTIONAL STRENGTH SKIN STRUCTURE DATA SUMMARY

Item	Description	Metal thickness, cm	Corrugation size		I_{theory}, cm^4 10^{-4}	I_{test}, cm^4 10^{-4}	$\frac{I_{test}}{I_{theory}}$	I_{theory}, single element, cm^4 10^{-4}	$\frac{I_{test}}{I_{theory}}$, single element	Conclusions
			Depth, cm	Pitch, cm						
4	Single element 	0.00381 0.00254 0.00381	0.17 0.269 0.475	0.353 0.820 1.08	0.524 0.878 4.24	0.53 0.89 4.26	1.01 1.01 1.0	0.524 0.878 4.24	1.01 1.01 1.0	Moment of inertia: $I_{theory} = I_{test}$
5	Single element with top skin 	0.00254 0.00254	0.190 0.353	0.381 0.698	1.0 3.3	0.424 1.42	0.424 0.43	0.437* 1.51*	0.97 0.94	No improvement over a single element.
6	Single element with top and bottom skins 	0.00254 0.00254	0.187 0.325	0.386 0.787	2.2 6.6	0.70 2.02	0.318 0.306	0.42* 1.28*	1.67 1.58	Approximately 60% improvement over single-element strength, but at the expense of a 48% increase in weight per unit strength.

*Does not include skin elements.

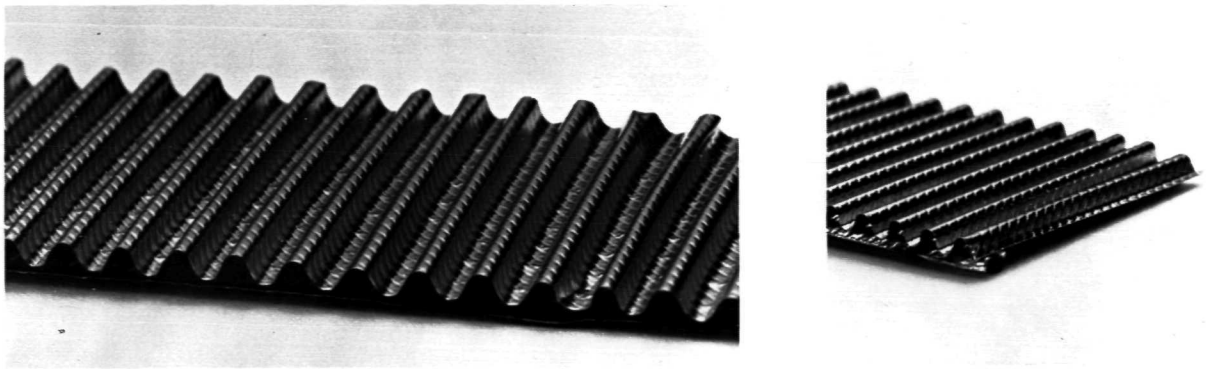

(a) 2.6 major corrugations per cm, .165 cm deep per element.

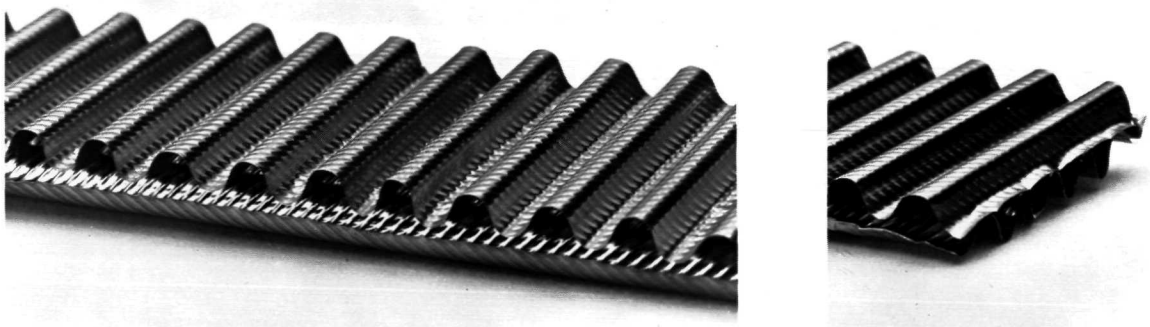

(b) 1.34 major corrugations per cm, .338 cm deep per element.

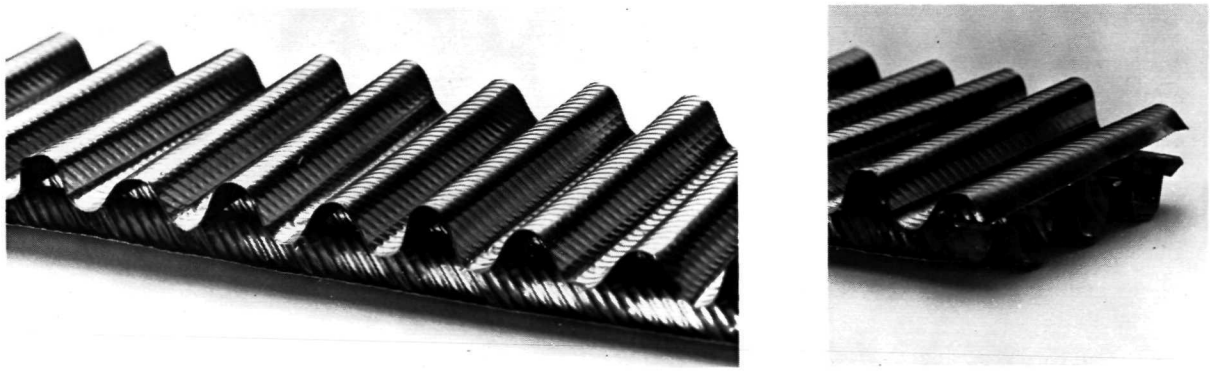

(c) .98 major corrugations per cm, .51 cm deep per element.

Note: (1) 9.84 micro corrugations per cm, .0038 cm deep, oriented at $\pi/4$ radian to major corrugations for each element.

(2) Major corrugations oriented normal to each other for each two-element laminate.

Figure 12. - Double-element omnidirectional structure assembly with major and micro corrugations aligned at $\pi/4$ radians.

TABLE III.– DOUBLE-ELEMENT STRUCTURAL ELEMENT SKIN SPECIMEN PARAMETERS

Item	Number of corrugations, cm	Corrugation depth, each element, cm	Metal thickness, cm
7	2.6	0.165	0.00254
8	1.34	0.338	0.00254
9	0.98	0.51	0.00254

The addition of a second element normal to the first does not add any bending stiffness. Therefore, the bending stiffness results without micro corrugations, as depicted in figure 13, are the same as those for a single element (figure 9).

The double-element configurations with micro corrugations aligned at $\pi/4$ radians to the major corrugations were also tested to experimentally determine the effect of micro corrugations on beam stiffness and the data are shown in figure 14. The data for the single element from which the double-element laminate was fabricated is also shown for comparison. The characteristics observed for the single element also extend to the laminate structure. It was shown previously that without micro corrugations, the bending stiffness was the same for a single element as for a double element. A review of the data, figure 14, taking into consideration data scatter, implies that the micro corrugations have not altered this relationship even though they do reduce the bending stiffness.

A double element with a center diaphragm was tested for stiffness to evaluate the effect of the center diaphragm. The configuration consisted of two corrugated beam elements oriented normal to each other with a center sheet metal diaphragm; it is described in table IV. The experimental results are presented in figure 15, and two-element data is given for comparison.

The increase in stiffness over the two-element system was consistent with values that would be predicted by reference to previous empirically obtained data; therefore, additional tests were not conducted for this configuration.

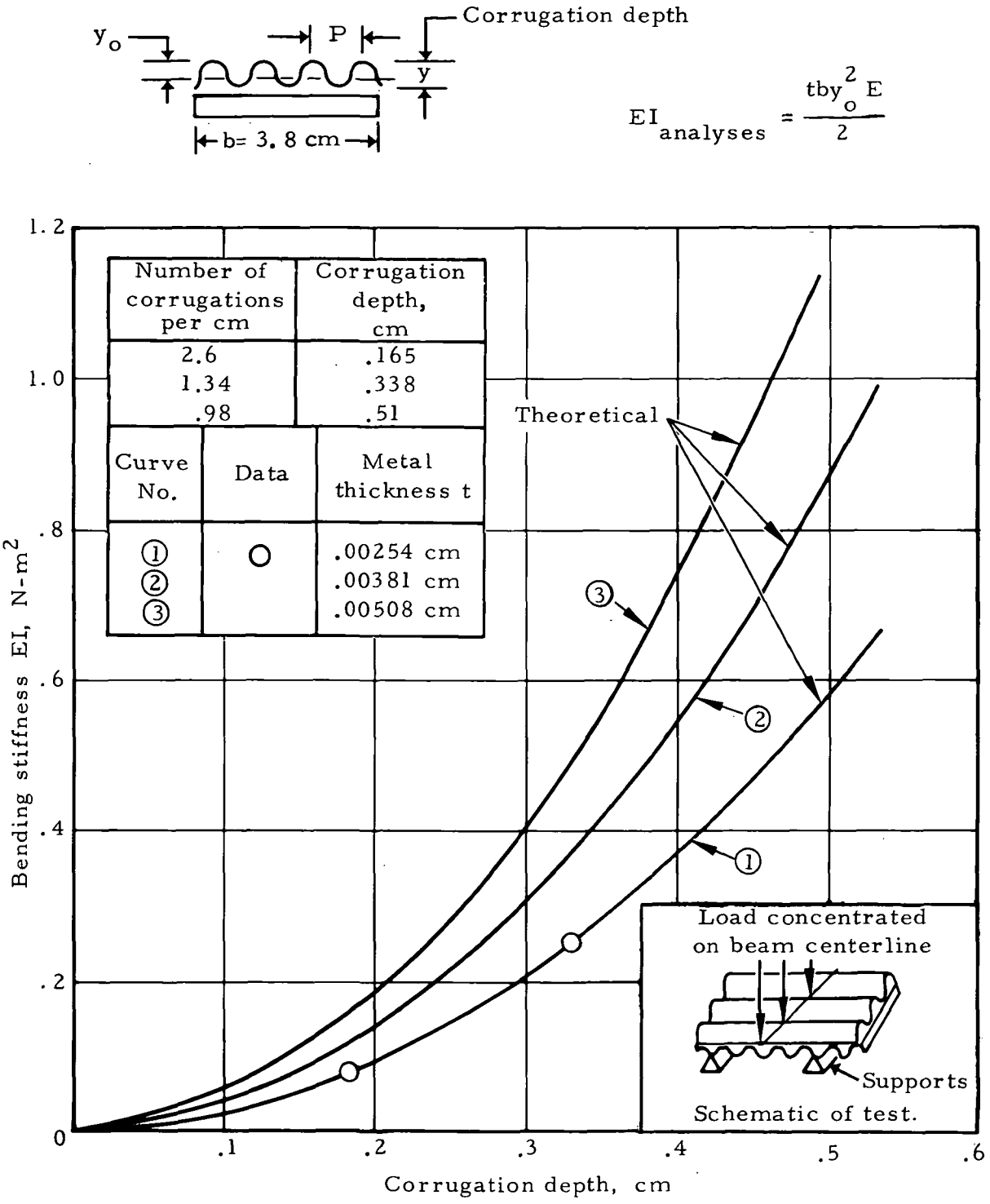

Figure 13. - Comparison of analytical and experimental beam stiffness for a double-element omnidirectional structure composed of corrugated beams without micro corrugations arranged normal to each other.

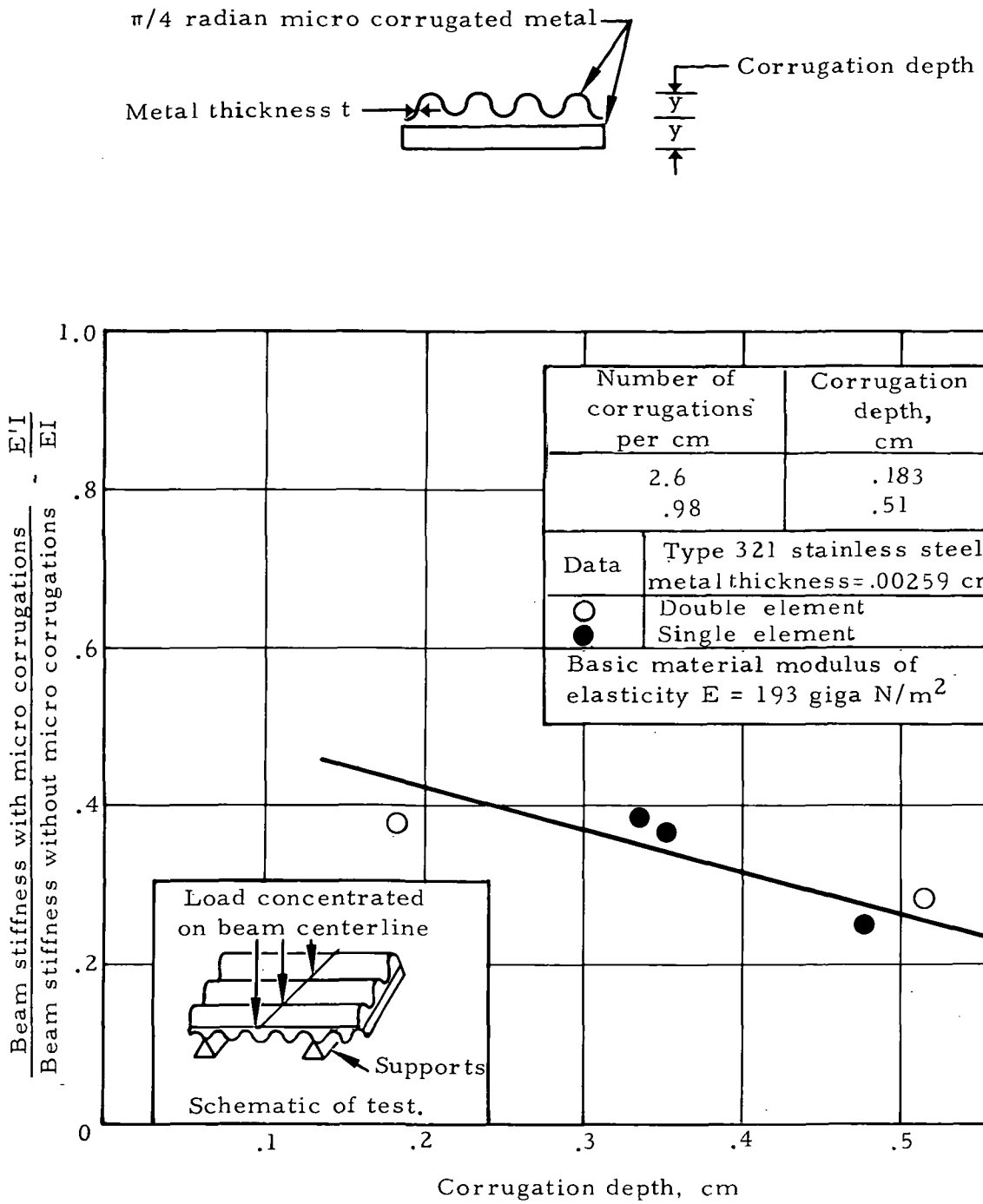

Figure 14. - Experimentally determined stiffness for a double-element omnidirectional corrugated beam laminate with the major strength elements aligned normal to each other.

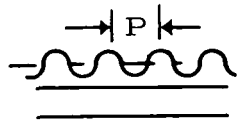

Double-element.

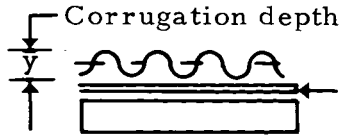

Double-element with center diaphragm.

All elements have $\pi/4$ radian micro corrugations.

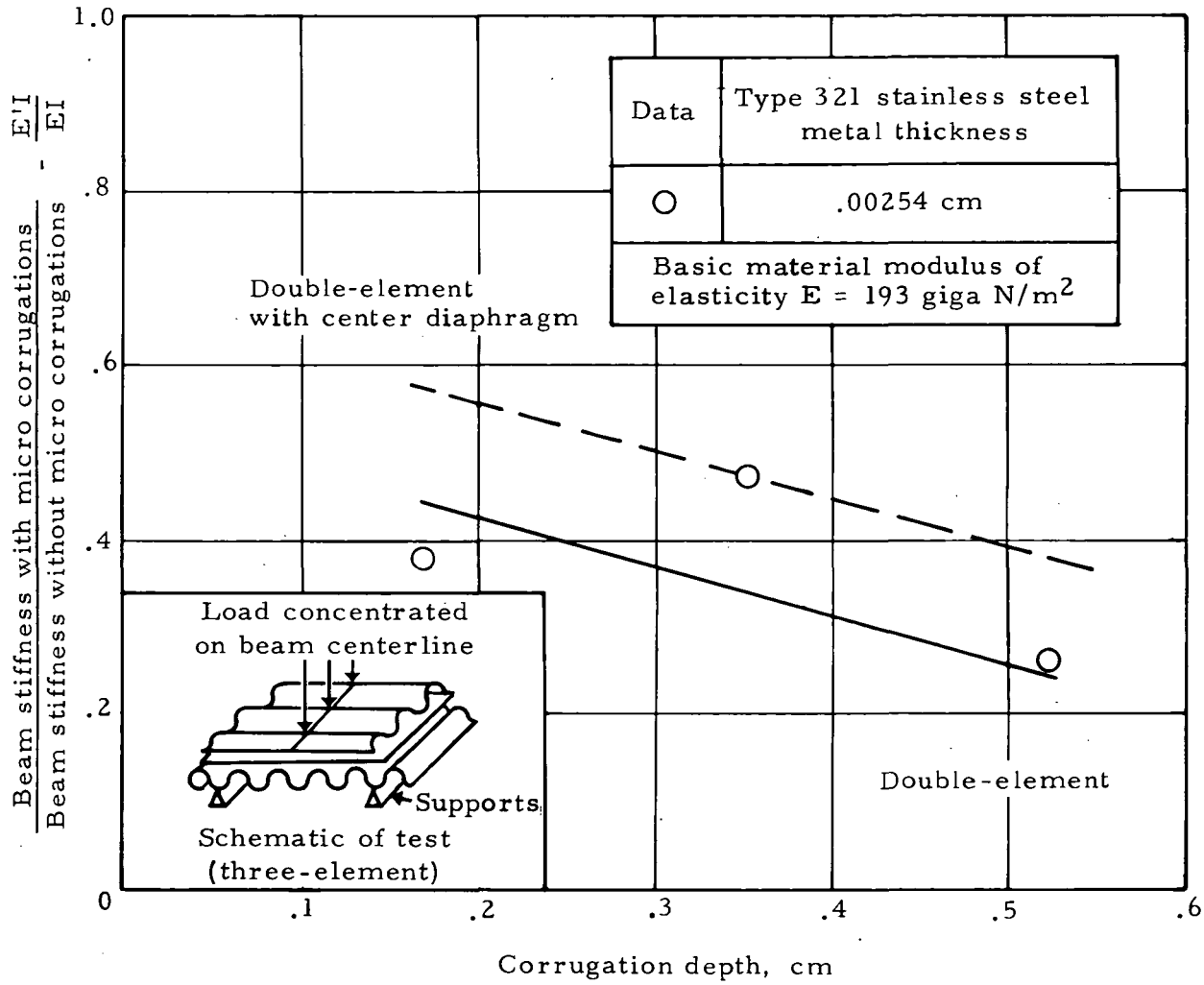

Figure 15. - Experimentally determined stiffness for a double-element omnidirectional structure composed of two corrugated beams arranged normal to each other with the addition of a center sheet metal diaphragm.

TABLE IV.– DOUBLE ELEMENT WITH CENTER DIAPHRAGM SKIN SPECIMEN PARAMETERS

Item	Element	Corrugation depth, cm	Corrugations per cm	Metal thickness, cm
10	Beams	0.338	1.34	0.00254
11	Center diaphragm	0.00381	Double-corrugated at 1.57 radians with 9.84 corrugations per cm	0.00127

Column Supports

Corrugated sheet metal was shaped into lineal support beams* for the unidirectional strength skin and circular hollow columns* for the omnidirectional strength skin. A metal thickness of less than 0.00254 cm was too fragile to effectively handle in fabrication, and a thickness greater than 0.00254 cm was not necessary for structural reasons; therefore, a majority of tests were performed with 0.00254 cm material.

Photographs of a typical lineal beam column test specimen and the test apparatus are presented in figure 16. The beam was bonded to the top and bottom structural plates, and two beam elements were used in the test item to provide stability in test. The top and bottom plates of the test item were guided in the compression test to ensure column loading.

The experimental results of the lineal beam column load tests are given in figure 17 for two end attachment designs. A plain end column without an integral normal bend (flange) was found to be superior in strength. Practical considerations of fabrication, however, dictate the use of the flange. The column support strength is in excess of requirements for optimum matching with skin structure; therefore, the structural degradation observed is not controlling in design.

Photographs of five corrugated metal hollow circular column supports are illustrated in figure 18. Column diameters of 5.08 cm, 8.9 cm, and 12.7 cm are shown for several corrugation depths and a metal thickness of 0.00254 cm. The tests were conducted with the same test technique used for the lineal beam columns. Column load capability as a function

*Patent applied for by Hughes Helicopters, division of summa corporation.

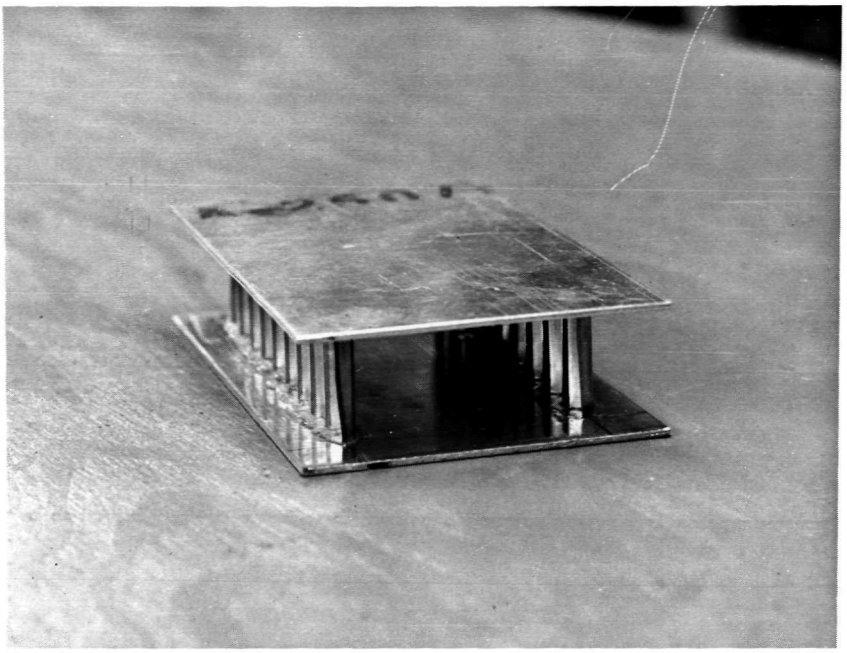

Typical lineal beam column test specimen - .00254 cm thick, type 321 stainless steel.

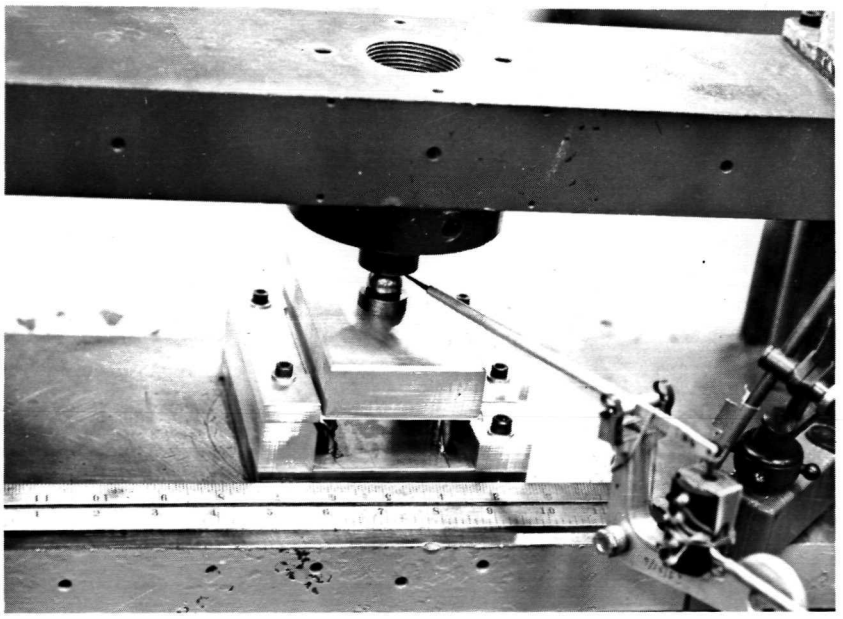

Test setup.

Figure 16. - Photographs of lineal beam column structural specimen and setup.

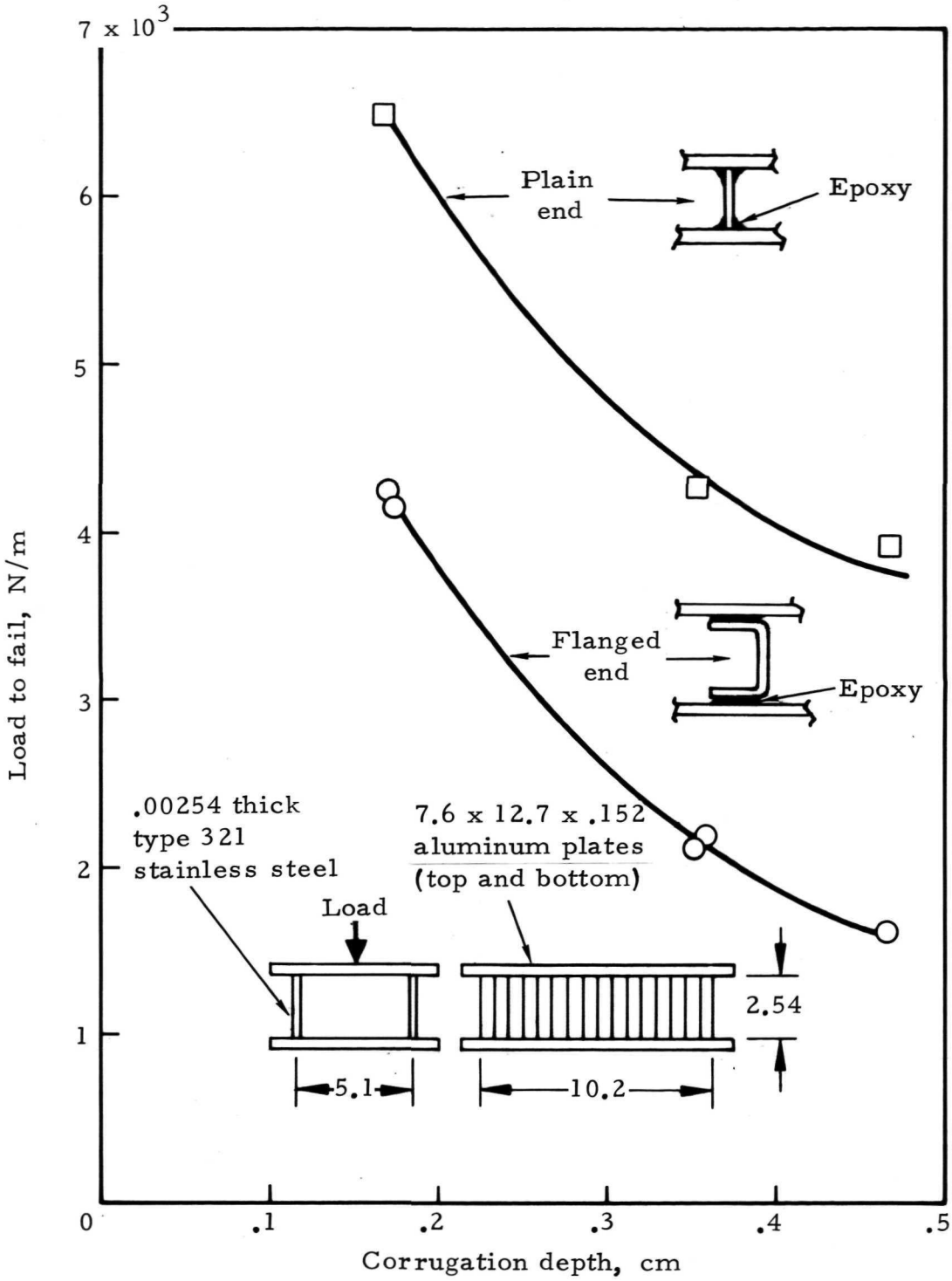

Note: All dimensions are in centimeters.

Figure 17. - Experimental maximum load capability of corrugated metal lineal beam columns.

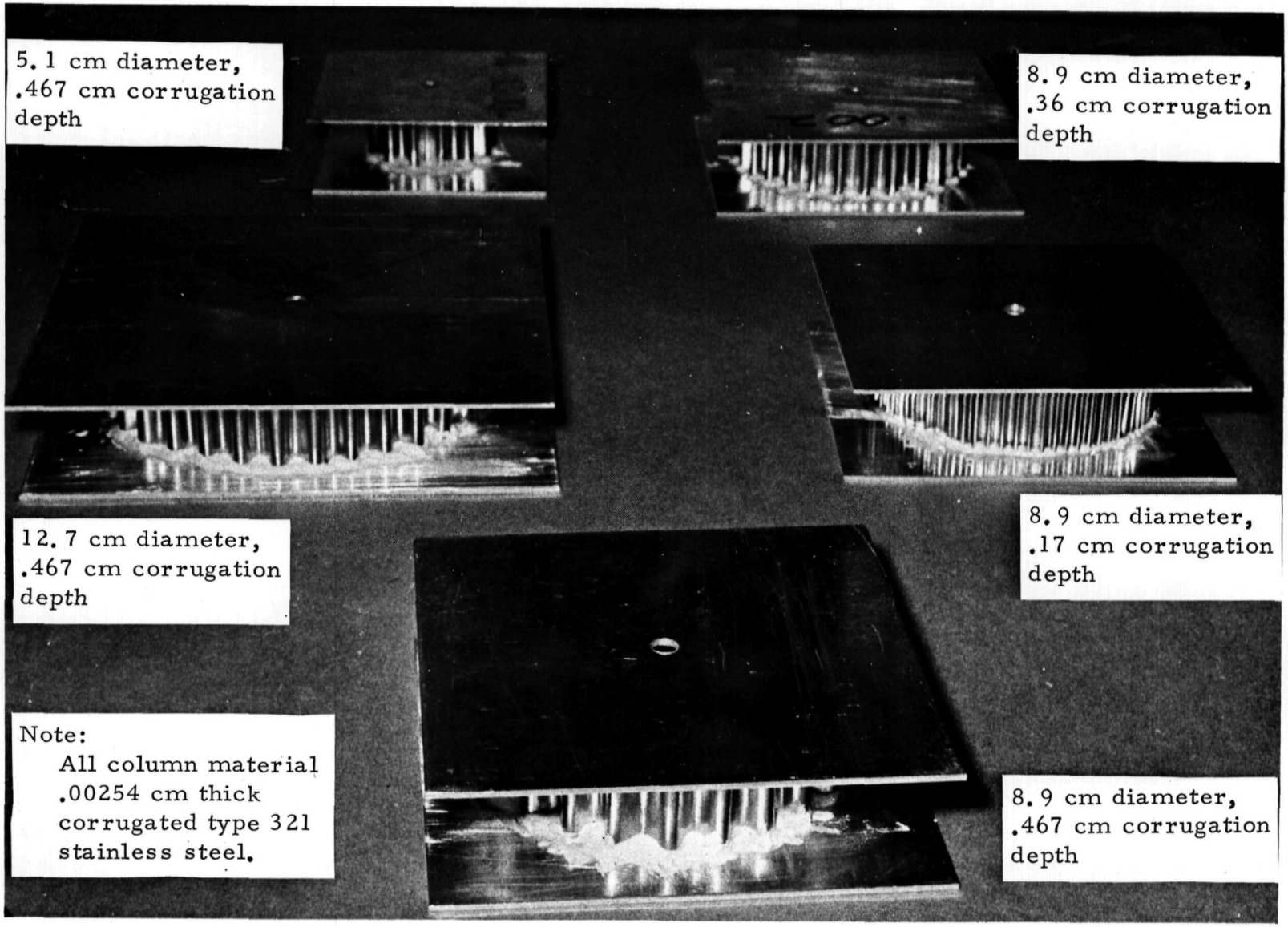

Figure 18. - Photographs of hollow column structural test specimens.

of corrugation depth was determined and is presented in figure 19 for 0.00254 cm thickness. Column strength was found to decrease with corrugation depth. The effect of column diameter is depicted in figure 20, where column load capability was observed to decrease with diameter.

The geometry of the systems tested is beyond established analytical formulae, primarily because thin sheet metal is employed. Increases in corrugation depth for such thin metal approach a straight (noncorrugated) section, and, similarly, smaller corrugations approach a flat sheet. An optimum for thin metal is most practically determined by considering fabrication limitations as well as the dictates of data trends.

PERFORMANCE COMPARISON OF GENERIC STRUCTURAL SYSTEMS

The experimental results were reviewed, and four of the most promising systems of structural skin and supports were selected for subsequent trade studies and optimization. Strength and weight comparisons were made of four generic systems of combined skin and supports. The configurations are shown in table V.

TABLE V.– DESCRIPTION OF THE FOUR SELECTED GENERIC SKIN AND SUPPORT SYSTEMS

Item	Generic configuration	Description of generic system
12	1	Single-element micro and major corrugated skin with a lineal corrugated beam support system.
13	2	Same as 1, except with an outer aerodynamic skin element transversely micro-corrugated 0.00381 cm deep, 9.84 per cm.
14	3	Circular hollow corrugated metal column support for a double-element cross-ply layup.
15	4	Same as 3, except lineal beams are used for support in an "egg-crate" pattern.

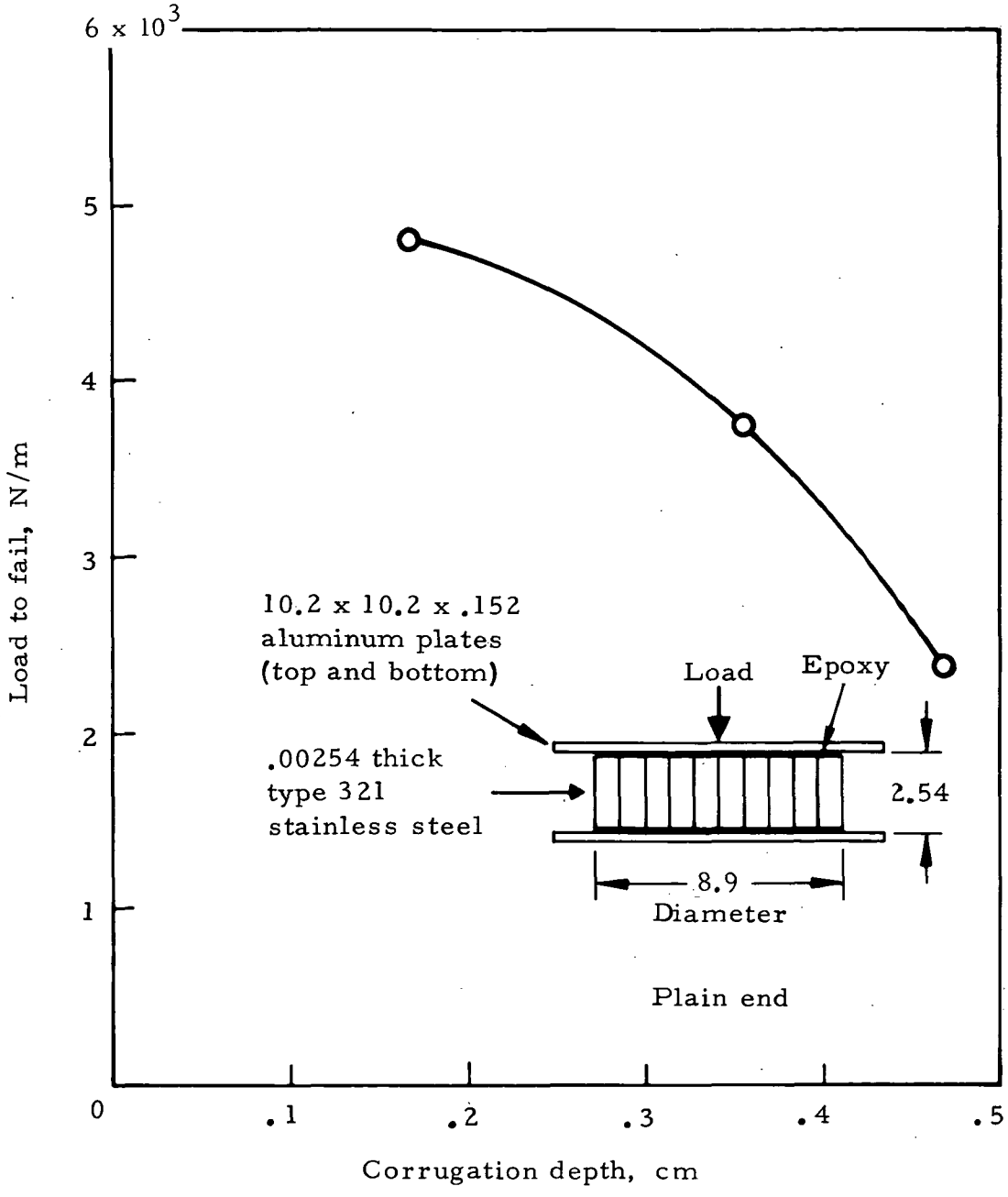

Note: All dimensions are in centimeters.

Figure 19. - Experimental maximum load capability of an 8.9 cm diameter corrugated metal hollow column.

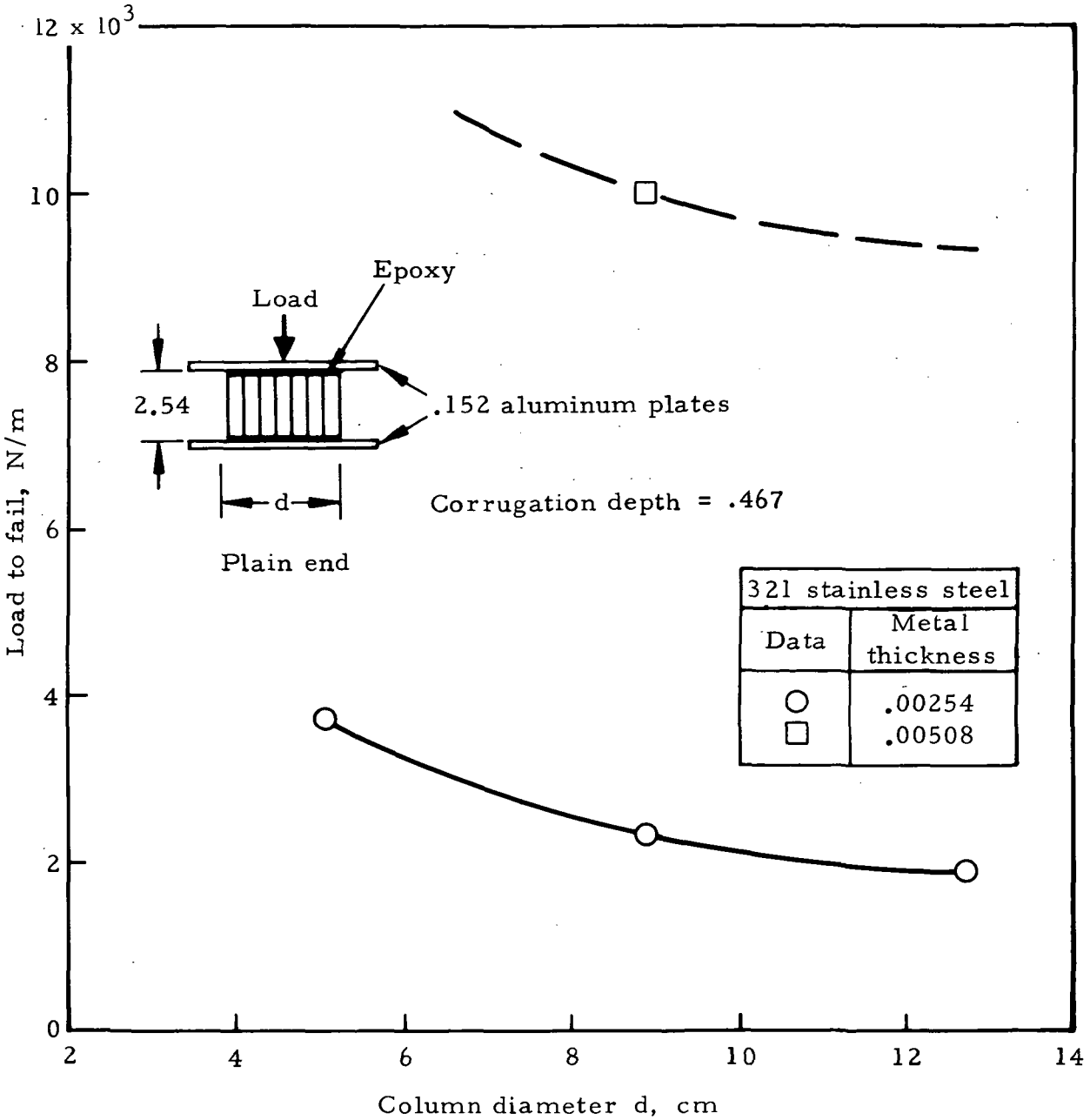

Note: All dimensions are in centimeters.

Figure 20. - Effect of column diameter and thickness on maximum load capability of a corrugated metal circular hollow column.

Aerodynamic load versus support span for the four configurations was analytically determined and is presented in figure 21. The support span spacing as a function of load for generic configurations 1 and 2 was determined by using the formula for a uniformly loaded beam fixed at both ends. The limiting allowable stress of 0.21 giga N/m^2 was attained before a maximum deflection of 0.30 cm was realized. Experimental test data showed that the aerodynamic skin did not increase the strength of a single element. Thus both configurations 1 and 2 have identical span/loading patterns, as shown in figure 21.

The theoretical variation between loading and span for generic configurations 3 and 4 was determined by first obtaining an equivalent thickness of a flat plate for the cross-ply layup using the section modulus formula for a beam. Then with this equivalent thickness, the cross-ply layup was stressed using the formula for a uniformly loaded flat plate with all edges fixed.

The aerodynamic load per kg/m^2 of structure is shown as a function of weight for a family of aerodynamic loads in figure 22. Generic configuration 1 was identified as the most efficient from a review of all data and the correlation shown in figure 22.

The thermal heat leak for the generic systems was analytically determined and correlated. Heat short per lineal meter of support structure for a range of metal thickness is presented in the table of figure 23, where column length per square meter of aerodynamic surface is shown plotted against aerodynamic load. Generic configuration 1 is also the most efficient in keeping the heat leak from the skin to the spacecraft surface to a minimum.

The more optimum generic configuration 1 was then parametrically evaluated, and aerodynamic load, support span, corrugation depth, and thermal short are correlated in figure 24. Weight is included in the correlation in figure 25, where the ratio of aerodynamic load/thermal short is varied with structure weight for a family of skin aerodynamic loads. The data is reduced to engineering application and may be used to establish a near-optimum design for selected service conditions.

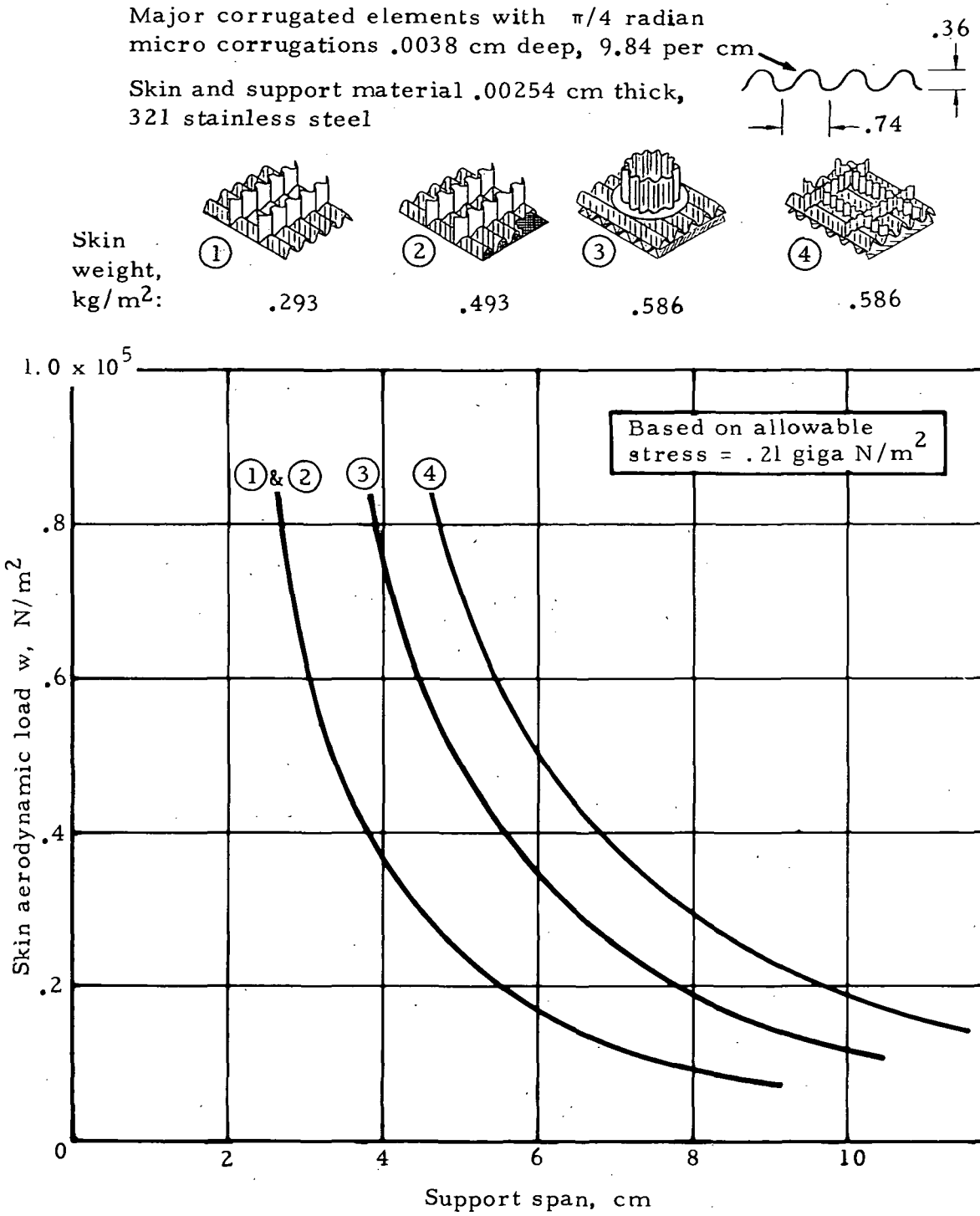

Figure 21. - Analytically derived strength comparison of generic structural systems.

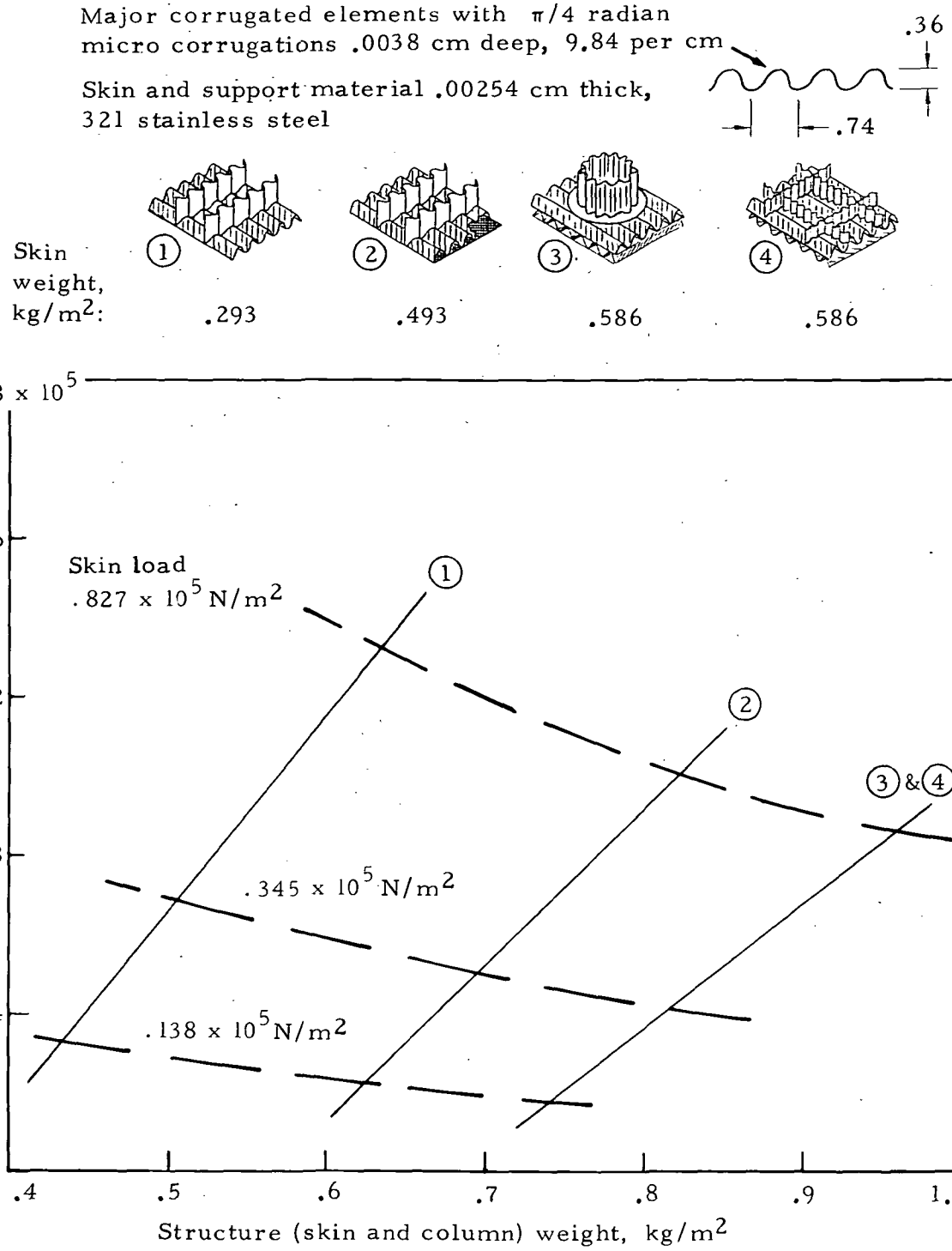

Figure 22. - Strength-to-weight analytic comparison of generic structural systems.

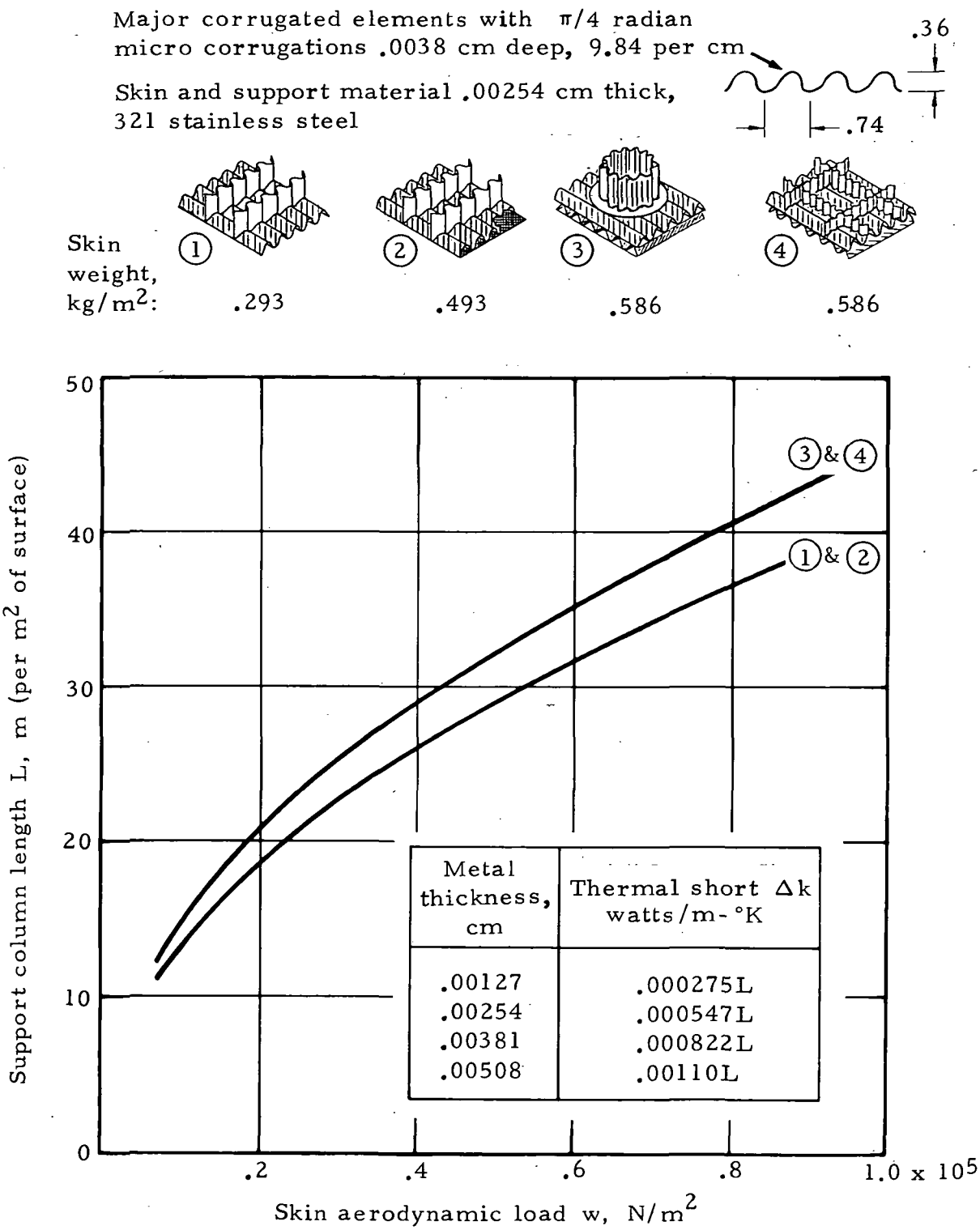

Figure 23. - Support length and thermal leak analytical comparison of generic structural systems.

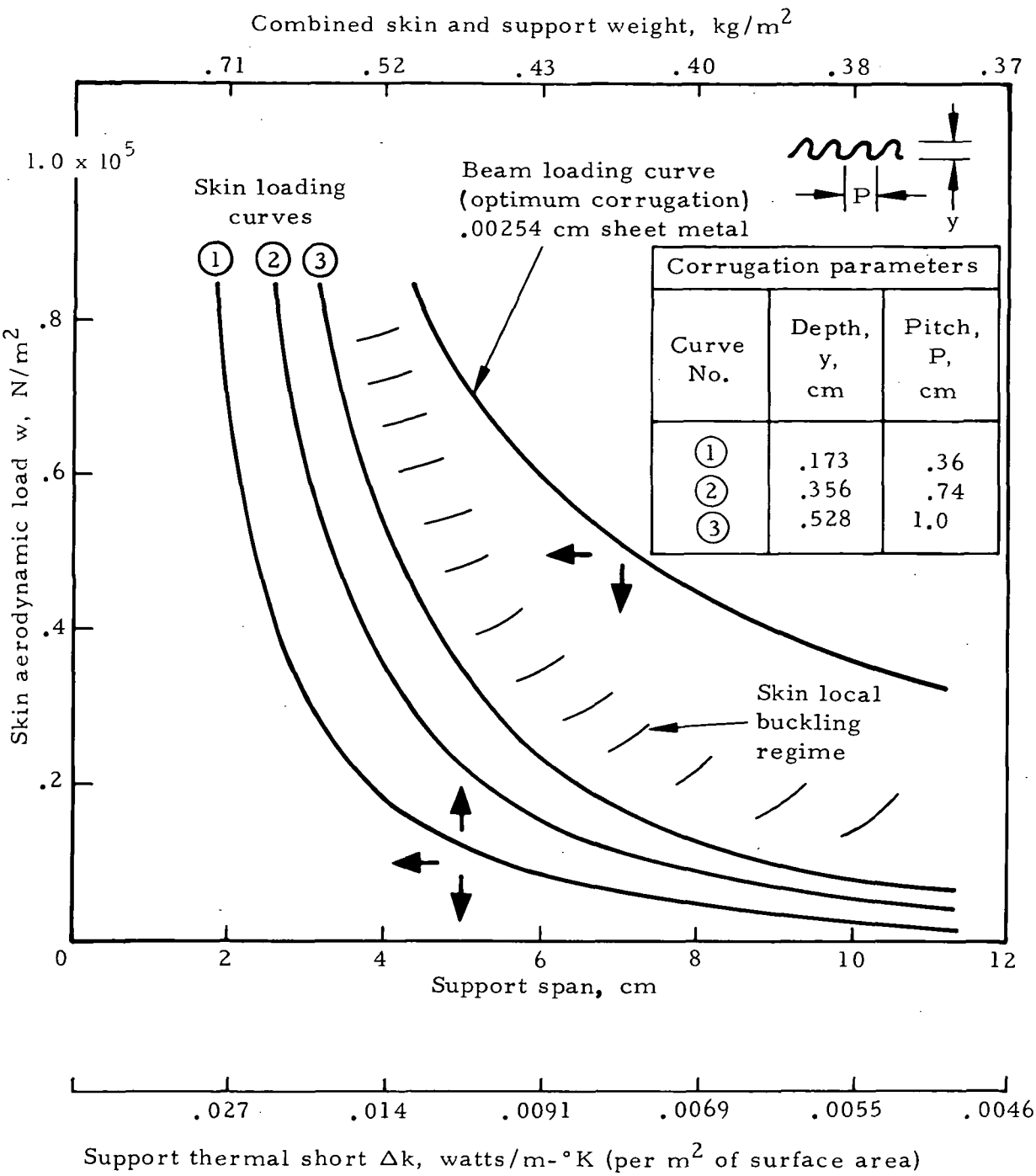

Figure 24. - Single-element unidirectional corrugated skin performance for a range of corrugation geometry. Beam column support capability shown for comparison.

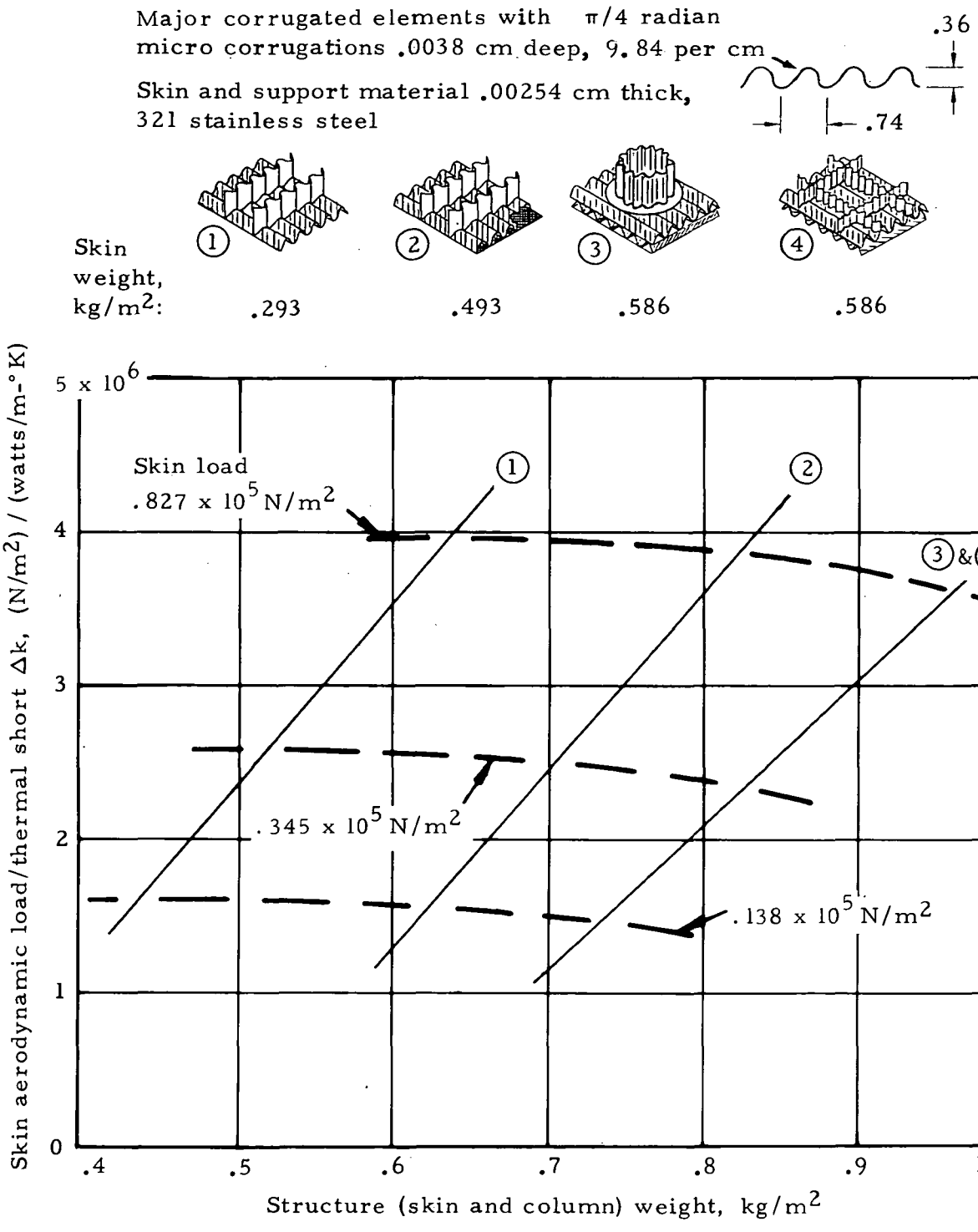

Figure 25. - Correlation of skin load, thermal short, and weight for generic structural systems.

SELECTED CONFIGURATIONS

Packaging and metal-wool insulation systems were selected and are described in the following paragraphs.

Packaging Structure

The experimental data and correlations show that a preferred structural configuration consists of a single-element skin and a lineal beam support system. Substantiating reasons for this selection are given below:

a. Easily fabricated, easily inspected

b. Minimum number of welds

c. Minimum weight

d. Minimum thermal leak

e. Can shape skin to extreme curvature in one dimension with no change in support beams

f. Double curvature feasible by notching or segmenting the lineal support beams

Two structural designs to package a 2.54 cm insulation for 0.35×10^5 N/m^2 and 0.25×10^5 N/m^2 aerodynamic loads are illustrated in figures 26 and 27 and described in table VI.

Metal Wool Insulation*

Several metal-wool insulation systems were designed and are described in table VII. These metal-wool systems may be combined with the two structural packaging configurations.

Selected Specimens

The packaged metal-wool systems prepared for arc jet testing are summarized in table VIII.

---

*LOW-Q™ metal wool insulation patent applied for by Hughes Helicopters, division of summa corporation.

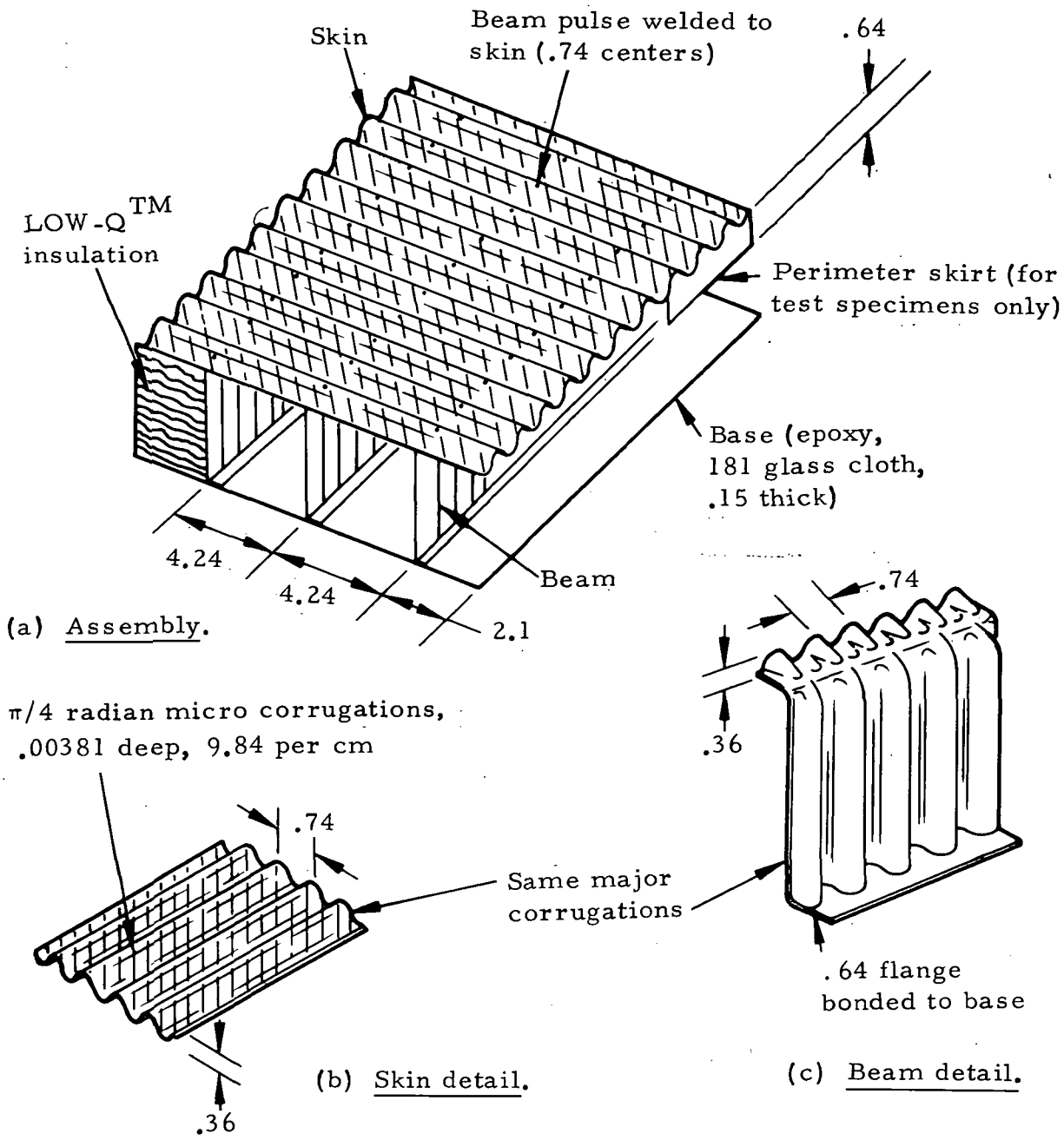

Note: Structural material .00254 thick, type 321 stainless steel.
All dimensions are in centimeters.

Figure 26. - Metal-wool heat shield structure, configuration A, single-element unidirectional skin with beam supports, 12.7 cm x 12.7 cm x 2.54 cm thick, 0.35×10^5 N/m^2 aerodynamic load.

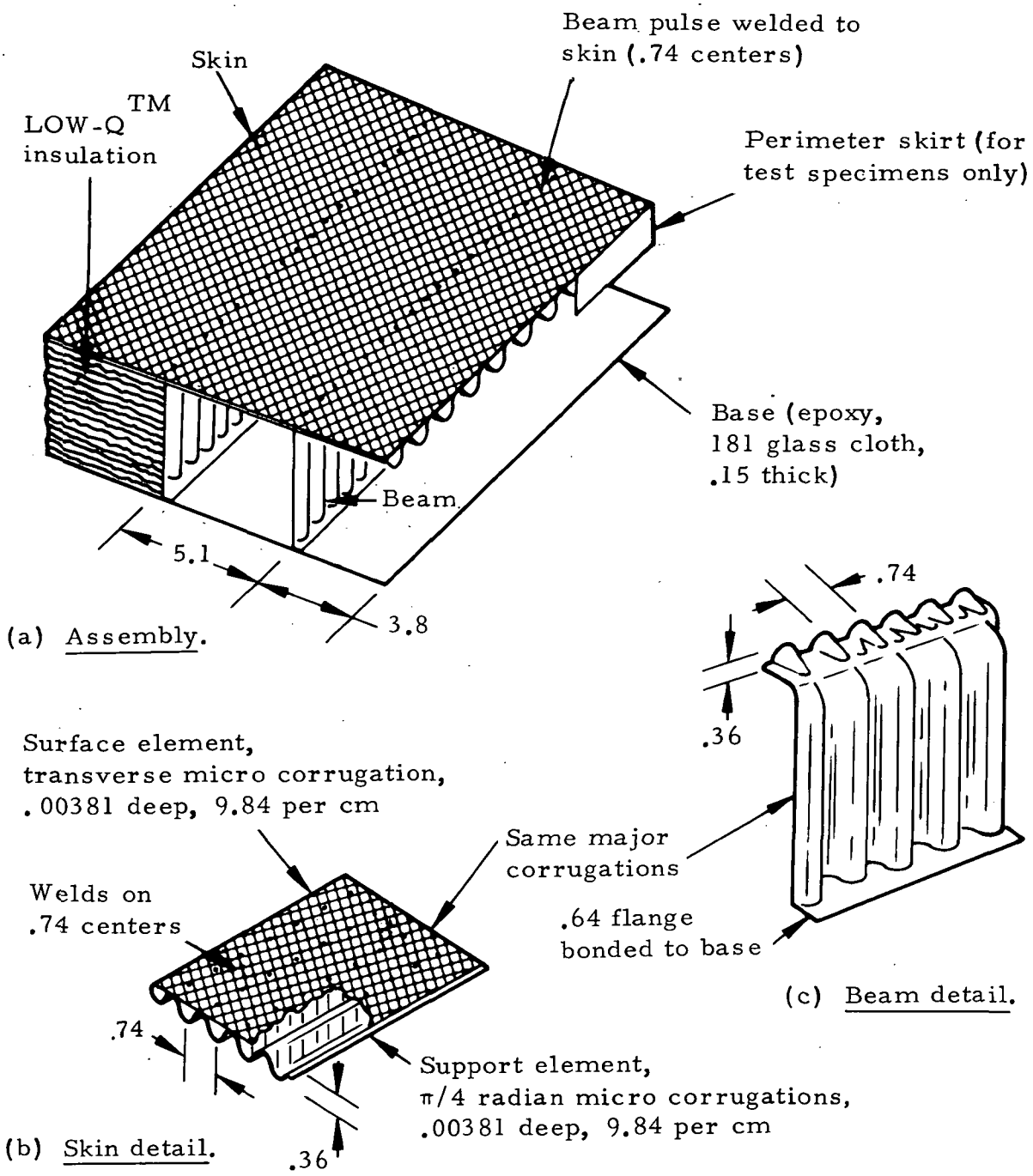

Note: Structural material .00254 thick, type 321 stainless steel.
All dimensions are in centimeters.

Figure 27. - Metal-wool heat shield structure, configuration B, double-element unidirectional skin with beam supports, 12.7 cm x 12.7 cm x 2.54 cm thick, 0.25×10^5 N/m^2 aerodynamic load.

TABLE VI.– SUMMARY OF DESIGN PARAMETERS FOR THE SELECTED PACKAGING STRUCTURES

Design parameters	Configuration A (figure 25)	Configuration B (figure 26)
Δk for one meter^2, W/m-°K	0.0136	0.0107
Δk for arc jet specimens, W/m-°K	0.013	0.0086
Skin weight, kg/m^2	0.293	0.488
Beam support weight, kg/m^2	0.186	0.146
Total weight, kg/m^2	0.479	0.634
Aerodynamic load capability, N/m^2 (based on an allowable stress of 0.21 giga N/m^2)	0.35×10^5	0.25×10^5

TABLE VII.– METAL-WOOL INSULATION FOR HEAT SHIELD STRUCTURES

Description (12.7 x 12.7 x 2.54 cm thick)	Wool				No. of radiation shields, 0.00127 thick stainless steel	Insulation criteria		k at 600°K, watts/m-°K	Rating factor, $k\rho_{wool}$, W-kg/m^4-°K
	Layers	Material	Filament diameter, microns	ρ, density, kg/m^3		Weight, kg/m^2	Density, kg/m^3		
Insulation No. 1--alternate layers of wool and shields	6	80/20 nichrome	8	40	5	1.52	59.8	0.066	2.64
Insulation No. 2--wool	–	80/20 nichrome	8	46.6	0	1.18	46.6	0.097	4.52
Insulation No. 3--alternate layers of wool and shields	6	347 stainless steel	8	36	5*	1.08	42.4	0.068	2.45
Insulation No. 4--alternate layers of wool and shields	6	347 stainless steel	4	32	5	1.31	51.7	0.061	1.95

*Optimized for 810°K service and lowest weight with aluminum radiation shields.

TABLE VIII. – COMBINED STRUCTURE/INSULATION ARC JET TEST SPECIMENS

Design and test parameters	Specimen number						
	1	2	3	4	5	6	7
	Configuration number (figures 26 and 27)						
	A-1	A-1	B-1	B-1	A-2	A-3	A-4
Maximum aerodynamic load, 10^5 N/m^2	0.35	0.35	0.25	0.25	0.35	0.35	0.35
Maximum hot face service:							
Sea level, °K	980	980	980	980	980	810	920
Space, °K	1370	1370	1370	1370	1370	810	1370
Packaged weight, kg/m^2	2.0	2.0	2.15	2.15	1.66	1.56	1.79
Packaged density, kg/m^3	78.7	78.7	84.7	84.7	65.4	61.4	70.5
Packaged thermal conductivity (k)*, W/m-°K	0.079	0.079	0.075	0.075	0.11	0.081	0.074
Material:							
Structure	321 stainless steel						
Wool	80/20 nichrome					347 ss	
Radiation shields	321 stainless steel				none	alum.	321 ss

*Reference: sea level, 810°K hot face.

PRODUCTION COSTS

A production cost estimate based on 1974 dollars was made for 465 square meters (5000 square feet) of metal-wool heat shield, 2.54 cm thick. The costs are summarized in table IX. The costs include quality control and packaging for shipment.

A 5.08 cm thickness is judged to cost less than $2150 per square meter ($200 per square foot).

TABLE IX.– PRODUCTION COSTS

Configuration no.	Estimated price		Estimated price per 465 meters^2 (5000 ft^2), $
	$ per meter^2	$ per foot^2	
A-1 (figure 26)	1625	151	755,000
B-1 (figure 27)	1927	179	895,000

CONCLUSIONS

Review of the study program permits the following summary observations and conclusions:

1. All-metal thermal insulation is a viable system for the thermal protection of airfoil and other aircraft surfaces. The objective of designing an efficient and reliable all-metal thermal barrier for shuttle application to areas which do not exceed 810°K has been met.

2. The fabrication of a metal packaging structure for metal-wool heat shields is practical, and manufacturing and assembly techniques have been demonstrated.

3. A double corrugated stainless steel skin structure was developed to accommodate thermal expansion in all directions when restrained at the edges.

4. The production costs of an all-metal system in a 2.54 cm thickness were estimated as $1625 per square meter ($151 per square foot).

5. Thermal conductivity of the metal system is less than the best competitive system when operating at space vacuum and equal to the best systems at atmospheric (sea-level) pressure. The packaged density of the metal system is less than the density of competitive systems for the same structural capability.

6. The temperature service of the 300 series stainless steel metal system extends to 1250°K for the shuttle surface due to the low oxygen concentration and low accompanying aerodynamic loads associated with the entry flight trajectory.

RECOMMENDED STUDIES

The current study successfully defined and substantiated a thermally efficient structure for packaging metal wool heat shields for Space Shuttle applications where temperatures do not exceed 1000°K at sea level or 1370°K in space. The service range and scope of an all-metal heat shield system may be increased after recommended investigations are performed.

Fatigue Testing

The examination of buffet and other loads consistent with selected modes of operation requires experimental evaluation. The positive results from the initial study indicate this to be a logical study phase.

Increased Load Capability

The thermal-expansion-controlled skin design technology demonstrated for aerodynamic loads of 0.35×10^5 newtons per meter^2 should be extended to thicker materials for more severe service. Design, fabrication, and testing of skin sections in the metal thickness range from 0.005 cm to 0.025 cm is recommended.

Fastening to Spacecraft

An optimized system for fastening metal heat shield structure to the spacecraft should be evolved. The study may include modifications to the spacecraft structure itself to arrive at a significant saving in systems weight.

Increased Heat Flux Capability

High heat loads (100-percent increase over systems tested) can be accommodated and structural capability maintained by utilizing refractory metal for portions of the structure and the metal-wool insulation systems provided a suitable coating can be developed for the refractory metal.

Low-Emissivity Structure and Insulation

A low-emissivity structure/insulation system may provide the solution to the lowest weight configuration for overall service at any altitude, and this type of system should be investigated.

APPENDIX A

METHODS FOR JOINING METAL HEAT SHIELD PANELS

The joining of a metal heat shield system to either a metal or a ceramic system was examined in the following design review.

Methods for Joining Metal Tiles or Metal Blankets in Situ

Six types of joints and three methods of sealing or fastening are schematically illustrated in figure 28. The six types of joints shown are as follows:

1. Simple overlapping
2. Compound overlapping
3. Hook
4. Corrugated overlapping
5. Bayonet
6. Flexible hinged

The three methods for joint sealing are as follows:

1. Use of RTV or similar mastic for low-temperature service.
2. Seam-welding of adjacent metal blankets or tiles utilizing a flexible hinged joint.
3. Seam-welding of any of the metal joints in place on the spacecraft.

The methodology of seam-welding in place has been demonstrated in preliminary studies conducted in support of the space shuttle prior to performance under this contract.

(1) Simple overlapping. (2) Compound overlapping. (3) Hook.

(4) Corrugated overlapping. (5) Bayonet.

Note: Above joints may or may not be sealed.
Seam weld for high temperature service.
Seal with RTV or equivalent for low temperatures.

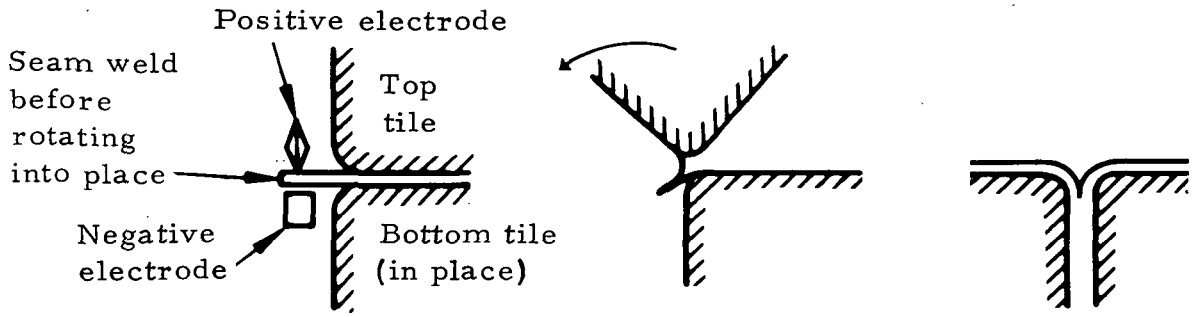

First step. Second step. Final step.

(6) Flexible hinged joint.

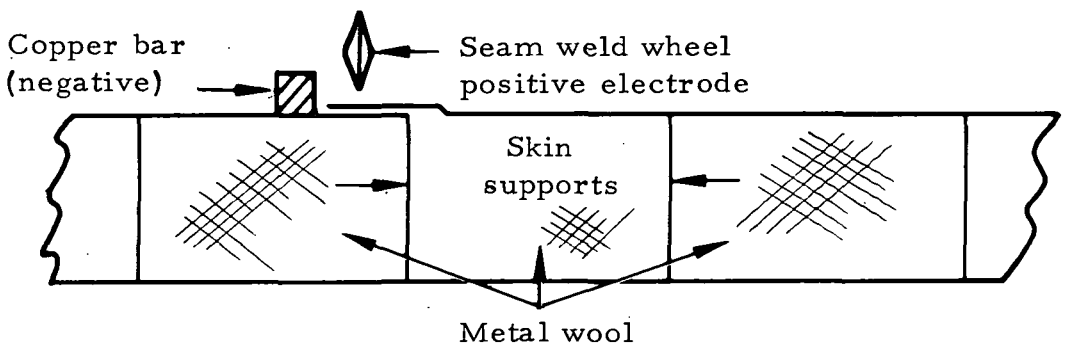

(7) Compound overlapped joint seam welded in situ.

Figure 28. - Methods of joining metal tiles or metal blankets in situ.

Methods of Joining Ceramic Tiles and Metal Insulation Systems

The fragile nature of ceramic tiles is not conducive to a joint of any kind; however, three possible joining techniques are schematically illustrated in figure 29. The three methods illustrated are:

1. An extension of the metal skin to seal the joint and also permit thermal expansion.

2. A metal-wool gasket joined to the structure with RTV or any suitable mastic.

3. A butt joint of metal-wool insulation and ceramic. The metal wool will allow for thermal expansion; however, the tolerance for chafing, fretting, or abrasion of the ceramic tile is not known.

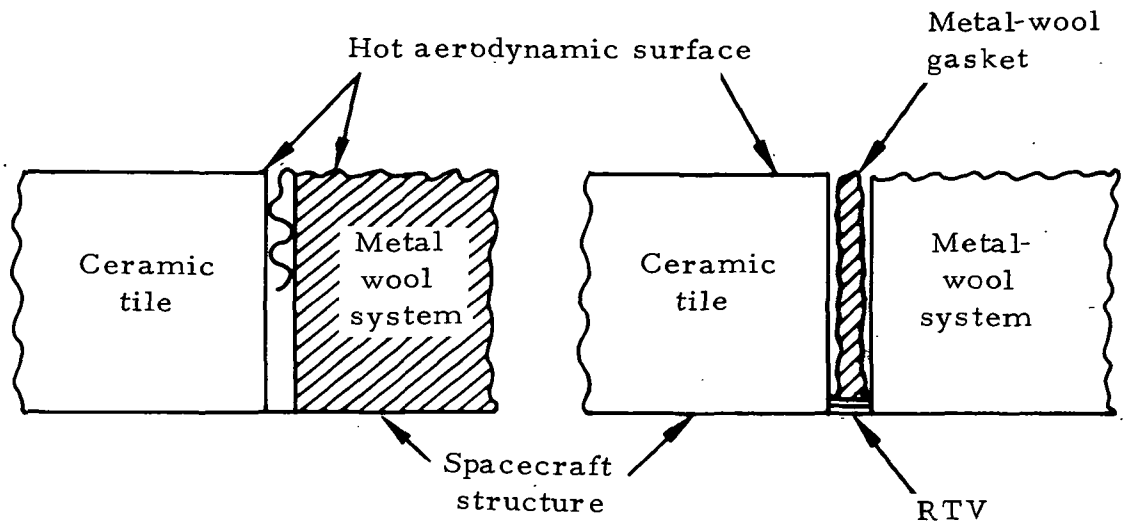

(1) Metal skin extended from outer surface into joint.

(2) Metal-wool gasket RTV bonded to structure.

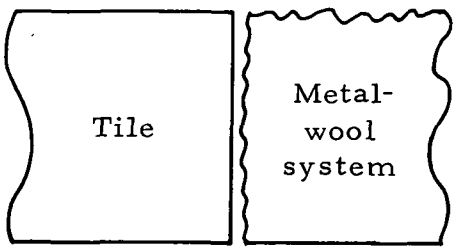

(3) Butt joint.

Figure 29. - Methods of joining ceramic tiles and metal insulation systems.

APPENDIX B

THERMAL SHORT REDUCTION METHODOLOGY

A good design places a thermal choke (or minimum area section) close to the heat source. This is illustrated schematically as a definition of good design practice in part (a) of figure 30.

Embodiments of this good design practice are applied to skin support configuration in part (b) of the figure, where arches or holes in the supporting corrugated foil structure are located near the hot surface of the system.

Similar holes or arches may feasibly be employed at the lower temperature end of a column of beam support to reduce weight without greatly reducing column strength. The actual reduction in strength as a function of opening size or location was not determined. These openings also facilitate rapid and complete venting of the system.

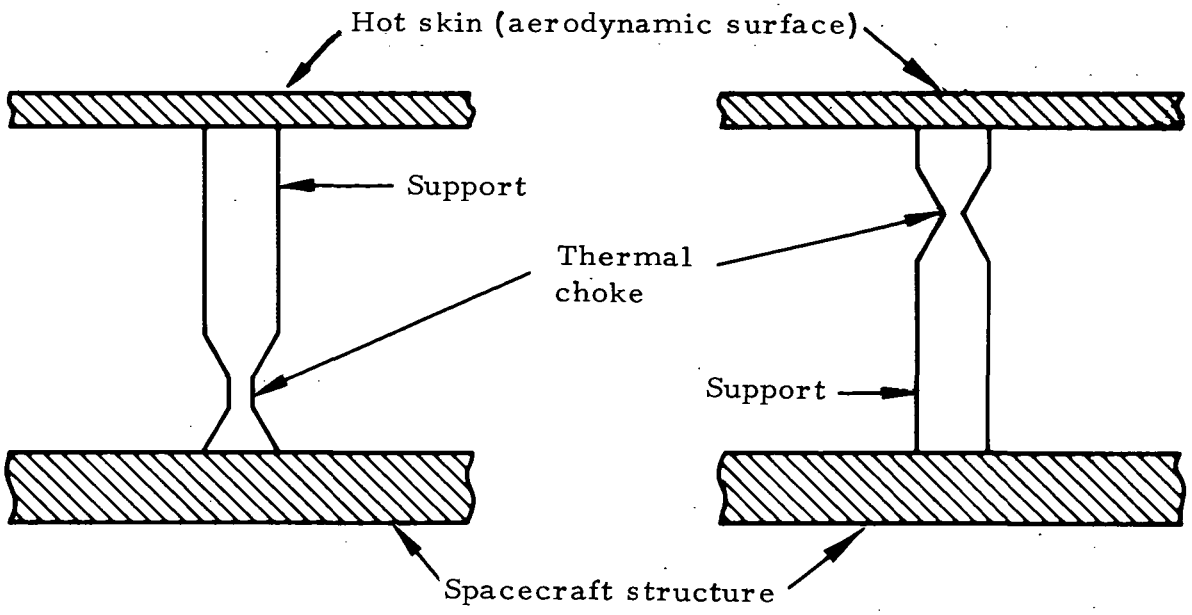

(a) Definition of good design practice.

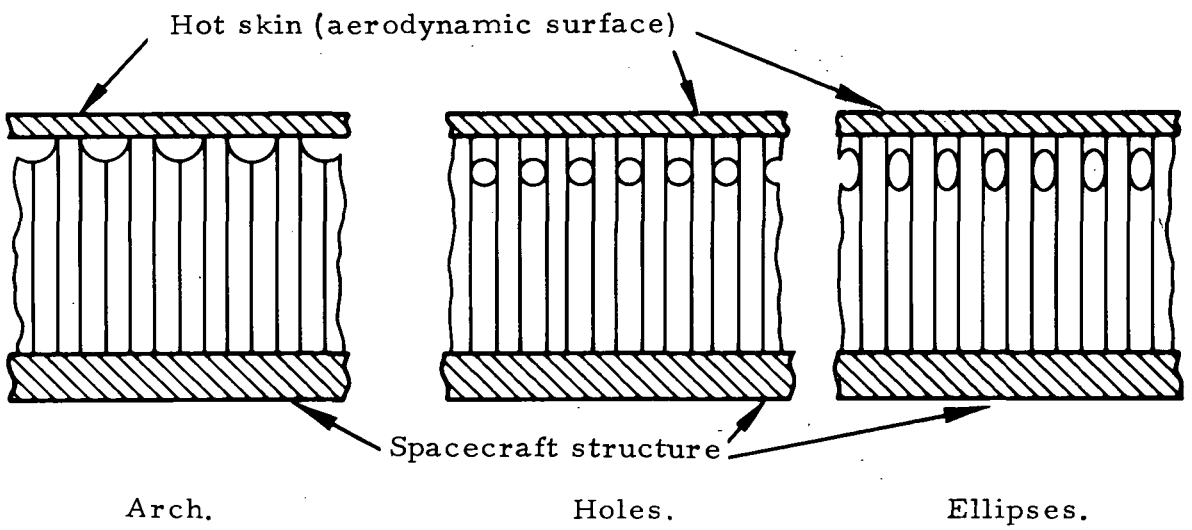

(b) Application of good design practice to skin supports.

Figure 30. Thermal short reduction methodology.

APPENDIX C

ANALYTICAL METHODS USED TO EVALUATE DESIGN AND CORRELATE DATA

Moment of Inertia

A theoretical moment of inertia of a sheet metal section with major strength corrugations was derived as shown in the following paragraphs. A three-point bending test was conducted to substantiate the analytical approach shown in figure 31. The section EI values were obtained from the test and I calculated inasmuch as the E of the material (stainless steel) was known.

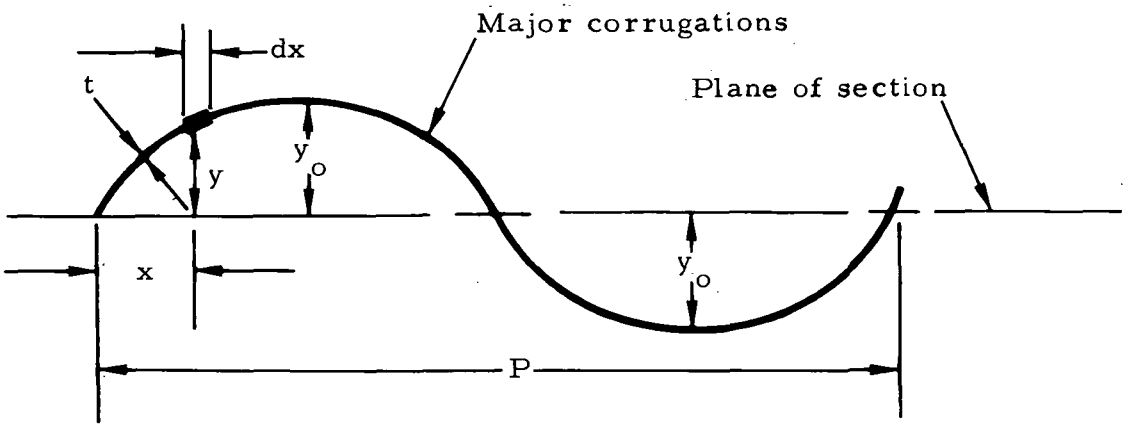

Figure 31. - Schematic of corrugated sheet system.

The corrugation pattern may be defined by the following sine-wave equation:

$$y = y_o \sin\left(\frac{2\pi x}{P}\right) \tag{C1}$$

The basic moment of inertia equation is as follows:

$$dI_P = y^2 t dx \tag{C2}$$

Combining (C1) and (C2),

$$dI_P = ty_o^2 \sin^2\left(\frac{2\pi x}{P}\right) dx$$

Integrating for a full cycle,

$$I_P = y_o^2 \frac{tP}{2\pi} \int_0^P \sin^2 \frac{2\pi x}{P} \, d\left(\frac{2\pi x}{P}\right)$$

$$= \frac{y_o^2 tP}{2\pi} \left[\frac{\left(\frac{2\pi x}{P}\right)}{2} - \frac{\sin 2\left(\frac{2\pi x}{P}\right)}{4} \right]_0^P$$

$$I_P = \frac{y_o^2 tP}{2} \tag{C3}$$

For n corrugations per inch, nP = 1 and

$$I_{\text{per inch}} = \frac{y_o^2 t}{2} \tag{C4}$$

and for width of beam = b,

$$I = \frac{y_o^2 tb}{2} \tag{C5}$$

Modulus of Elasticity

Analysis may be used to define corrugated thin sheet metal section properties; however, the addition of a second corrugation oriented at $\pi/4$-radian azimuth displacement in the same structure was found to be beyond analytical definition. Several specimens 3.8 cm wide and 15.2 cm long were prepared and tested as simply supported beams both with and without micro corrugations. The specimens without micro corrugations were found to agree with accepted theory, and the section EI value could be predicted satisfactorily. The EI values of the micro-corrugated specimens were determined experimentally to establish the "effective" modulus of this type of section.

REFERENCES

1. Goldstein, Howard E.; John D. Buckley; Harry M. King; Hubert B. Probst; and Ivan K. Spiker: Reusable Surface Insulation Materials Research and Development. NASA Space Shuttle Technology Conference - Dynamics and Aeroelasticity, Structures and Materials, NASA TM X-2570, pp. 373-433.

2. Miller, R. C.: LOW-Q(tm) Thermal Insulation — Technical Information for Spacecraft and Aircraft Applications. Report HH 73-61, Hughes Helicopters, September 1973.

3. Anon.: Final Letter Report — Muffs and Cuffs for UH-1 Exhaust Deflector. Report HHC 73-13, Hughes Helicopters, January 1973.

4. Miller, R. C.; and J. L. Clure: In-Side Out Duct Aluminum Structure Experimental Substantiation at 1800°F. Report HH 73-71, Hughes Helicopters, October 1973.

5. Anon.: Metric Practice Guide. E380-72, Amer. Soc. Testing Mater., June 1972.